



# A new framework for the simulation of equation-based models with variable structure

Dirk Zimmer

## Abstract

Many modern models contain changes that affect the structure of their underlying equation system, e.g. the breaking of mechanical devices or the switching of ideal diodes. The modeling and simulation of such systems in current equation-based languages frequently poses serious difficulties. In order to improve the handling of variable-structure systems, a new modeling language has been designed for research purposes. It is called Sol and it caters to the special demands of variable-structure systems while still representing a general modeling language. This language is processed by a new translation scheme that handles the differential-algebraic equations in a highly dynamic fashion. In this way, almost arbitrary structural changes can be processed. In order to minimize the computational effort, each change is processed as locally as possible, preserving the existing computational structure as much as possible. Given this methodology, truly object-oriented modeling and simulation of variable-structure systems is made possible. The corresponding process of modeling and simulation is illustrated by two examples from different domains.

## Keywords

variable-structure systems, equation-based modeling, differential-algebraic equations, index reduction

## 1. Introduction

Modern modeling methodologies in the field of physical systems are increasingly based on equation-based modeling languages. Such languages have a declarative character and are based on differential-algebraic equations (DAEs). Furthermore, they feature various object-oriented constructs that enable a proper organization of knowledge. In this way, models can be built up hierarchically and composed out of submodels belonging to various domains.

Nowadays, the most prominent equation-based language is Modelica.<sup>1,2</sup> It was designed in the late 1990s by an international standardization committee. A number of companies have meanwhile adopted the Modelica technology. Large-scale system models, e.g. describing the dynamics of cars, consisting of several hundreds of thousands of lines of code have been encoded in this language. These models have proven to be as run-time efficient as the best manually encoded models of the past. Nevertheless, there are also other languages that feature equation-based modeling. For instance VHDL-AMS<sup>3</sup> or gPROMS<sup>4</sup> are being used in industry. Smaller languages such as Chi<sup>5,6</sup> serve academic interests.

Unfortunately, many of these languages share a common deficiency. They suppose a fixed computational

structure of the resulting model and, hence, the support of variable-structure systems is very limited. However, many contemporary models contain structural changes at simulation run-time. The motivations for these models are manifold:

- The structural change is caused by ideal switching processes. Classic examples are ideal diodes in electric circuits and rigid mechanical elements that can break apart.
- The model features a variable number of variables: this issue typically concerns social or traffic simulations that feature a variable number of agents or entities, respectively.
- The variability in structure is to be used for reasons of efficiency: a bent beam should be modeled in

---

German Aerospace Center, Institute of System Dynamics and Control,  
Weßling-Oberpfaffenhofen, Germany

### Corresponding author:

Dirk Zimmer, German Aerospace Center, Institute of System Dynamics  
and Control, Münchner Strasse 20, D-82234 Weßling-Oberpfaffenhofen,  
Germany.

Email: dirk.zimmer@dlr.de

more detail at the point of the buckling and more sparsely elsewhere.

- The variability in structure results from user interaction: when the user is allowed to create or connect certain components at run time, this usually results in a structural change.

Evidently, the collective term variable-structure systems is very general and can be applied to various modeling paradigms such as agent-simulations or finite-element meshes. In this paper, we focus on the modeling within object-oriented equation-based languages for multi-physics systems (e.g. Modelica<sup>1,2</sup> or gPROMS<sup>4</sup>). In order to obtain a more precise picture for the particular problems in this domain, let us look at a suitable example: the trebuchet.

### 1.1. The trebuchet

The trebuchet is an old catapult weapon developed in the middle ages. It is known for its long range and its high precision. Figure 1 depicts a trebuchet and presents its functionality. It is a seemingly simple system but its simulation involves severe structural changes on a higher-index system (see Sections 4 and 5). Technically, the system can be described within planar mechanics and it is a double pendulum propelling a projectile in a sling. The rope of the sling is released on a predetermined angle  $\gamma$  when the projectile is about to overtake the lever arm. Furthermore, the following assumptions hold true for the modeling:

- All mechanics are planar. The positional states of any object are therefore restricted to  $x$ ,  $y$ , and the orientation angle  $\varphi$ .
- All elements are rigid. Also the sling is non-elastic.
- The rope of the sling is ideal and weightless. It exhibits an inelastic impulse when being stretched to maximum length.
- The revolute joint of the counterweight is limited to a certain angle  $\beta$  (in order to prevent too heavy back-swinging after the projectile's release). It also exhibits an inelastic impulse when reaching its limit.

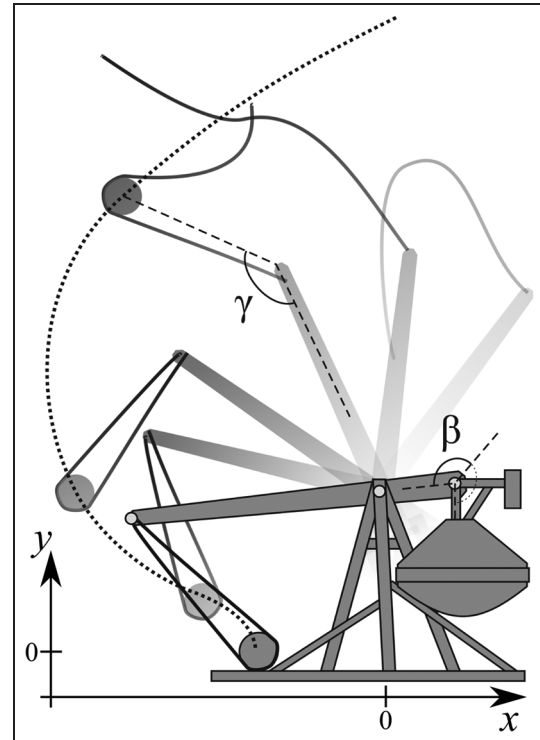


Figure 1. Functionality of a trebuchet.

Whereas these idealizations simplify the parameterization of the model to a great extent, they pose serious difficulties for a typical simulation environment of an equation-based language. This ideal modeling leads to various structural changes that occur during the simulation of the system. At  $t = 0.5$  s, one of these changes is recognizable in the trajectory of the projectile (Figure 2) as discrete change of the first time derivative.

### 1.2. Modeling the trebuchet

The most direct approach is to model the system as a whole. In modern object-oriented modeling environments

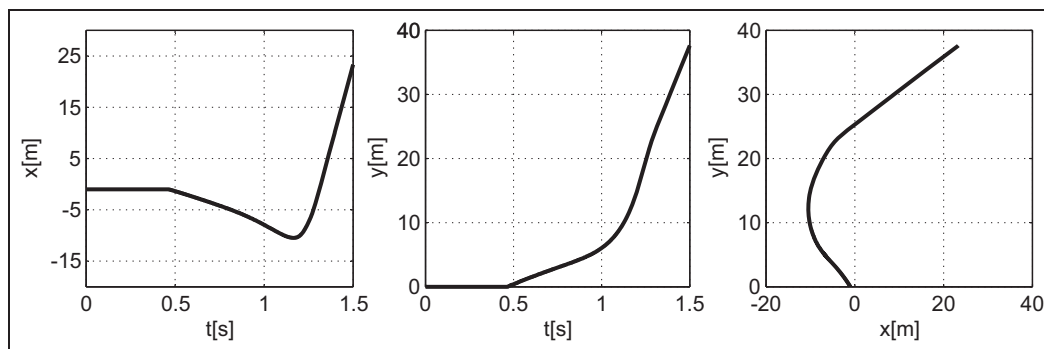
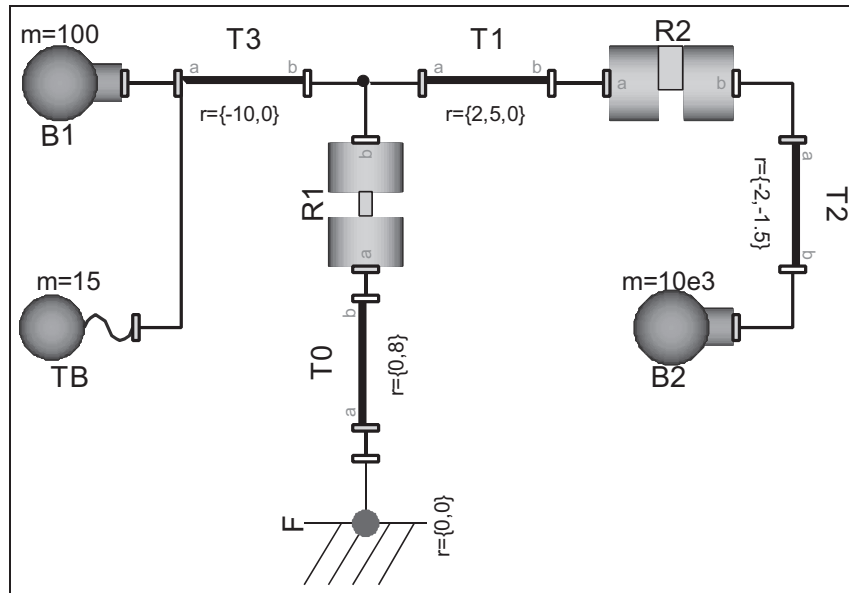


Figure 2. Trajectory of the projectile.



**Figure 3.** Model diagram of the trebuchet.

such an approach is still possible but certainly unfavored. The resulting model would be highly complex and none of its parts could be properly reused. For another mechanical system, the modeling would have to be redone from scratch again.

Instead, the system is composed out of individual components that form a model library and interact with each other by a common interface. For this example, the following components suffice:

- one fixation component (F);
- four fixed translations (T0, T1, T2, T3);
- one revolute joint (R1);
- one limited revolute joint (R2);
- two bodies with mass and inertia (B1, B2);
- one ideal rope with a body attached to it (TB).

The assembly of the system from these components is represented by the model diagram of Figure 3. In the next step, we have to assign a correct set of equations to each component. Let us look at the equations for the simple revolute joint:

$$\begin{aligned}\varphi_2 &= \varphi_1 + \varphi_{R1} \\ x_2 &= x_1 \\ y_2 &= y_1 \\ f_{x,1} + f_{x,2} &= 0 \\ f_{y,1} + f_{y,2} &= 0 \\ t_1 + t_2 &= 0 \\ t_2 &= 0\end{aligned}$$

These equations relate the interface variables of the component. These are the variables that represent the position:  $x$ ,  $y$ , and the angle  $\varphi$ . The second set describes the force and torque  $f_x$ ,  $f_y$ , and  $t$ . The interface variables are indexed by subscripts 1 or 2 according to which of the two interfaces they belong to.

The angle  $\varphi_{R1}$  of the revolute is not the sole variable of interest; also its velocity  $\omega_{R1}$  and acceleration  $\alpha_{R1}$  can be helpful variables for the simulation of mechanical systems. Hence the set of equations is extended by the following two *differential* equations:

$$\begin{aligned}\omega_{R1} &= \dot{\varphi}_{R1} \\ \alpha_{R1} &= \dot{\omega}_{R1}\end{aligned}$$

The trebuchet contains not only a simple revolute joint, but also a version with a limited range that is similar in its functionality to an elbow. The corresponding model can be described by two major modes: *free* or *fixated*. The mode free is equivalent to a normal revolute joint whereas the mode equals a fixed orientation in the fixated mode. The transition between these modes is triggered when the angle of the revolute exceeds a predetermined limit  $\beta$ . Since this transition causes a discrete change in velocity, it involves an inelastic impulse on the rigidly connected components. Furthermore impulses from other components (such as for instance the ideal rope) need to be handled as well in this component. The different modes and their transitions are presented in the graph of Figure 4, where the continuous-time modes are depicted as round boxes and the rectangular boxes denote intermediate modes that cause discrete (immediate) changes in the value of variables.

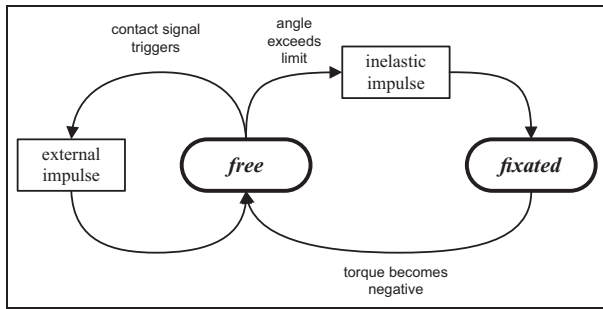


Figure 4. Mode-transition graph of the limited revolte.

Table 1. Transition from free to fixated mode.

Free		Fixated			
$\varphi_2$	=	$\varphi_1 + \varphi_{R2}$	$\varphi_2$	=	$\varphi_1 + \beta$
$x_2$	=	$x_1$	$x_2$	=	$x_1$
$y_2$	=	$y_1$	$y_2$	=	$y_1$
$f_{x,1} + f_{x,2}$	=	0	$f_{x,1} + f_{x,2}$	=	0
$f_{y,1} + f_{y,2}$	=	0	$f_{y,1} + f_{y,2}$	=	0
$t_1 + t_2$	=	0	$t_1 + t_2$	=	0
$t_2$	=	0			
$\omega_{R2}$	=	$\dot{\varphi}_{R2}$			
$\alpha_{R2v}$	=	$\ddot{\omega}_{R2}$			

The modeling of variable-structure systems by different modes cannot be achieved by a pure equation-based modeling in a convenient manner. The modeling of different modes and their transition needs to be considered as well. Furthermore events need to be described that trigger the transition. In addition, equations for the impulse behavior of the system need to be formulated. In order to be concise, we omit these aspects here and focus only on the structural change between the continuous-time modes. Here, each mode has its separate set of equations.

The difference between these two modes is presented in Table 1. The variables  $\varphi_{R2}$ ,  $\omega_{R2}$ ,  $\alpha_{R2}$  cease to exist in the fixated mode and, therefore, there are three fewer equations in the corresponding set of equations. Five of the remaining six equations are shared by both modes and, thus, the structural change concerns only a subset of the total modeling equations.

We see that we can represent this structural change by a simple modification in a set of DAEs. Thus, it may initially seem surprising that such an easy model cannot be realized within current equation-based languages for physical systems. Although the structural change may seem trivial for the individual component, it is severe for the complete model of the trebuchet. It changes the number of continuous-time states and leads to different algebraic equations systems. The index reduction of the DAE systems requires the automatic differentiation of certain model equations (see Section 5). Depending on the

continuous-time mode of the limited revolte, different equations need to be differentiated.

The situation is even more complicated, when we consider that the limited revolte joint is not the only component of the trebuchet that causes structural changes. The component for the torn body introduces another three independent continuous-time modes:

1. The body is at rest as long as the rope has not been stretched.
2. The body represents a pendulum as long as the release angle  $\gamma$  has not been reached.
3. The body is free.

For each of these modes, different variables are used to describe the positional state of the body. In the first mode, the position is constant and the model contains no state variables. In the second mode, the angle and angular velocity define the positional states, whereas the body is free in the last mode and consequently defines the maximum of six state variables.

There are three components that define all state variables of the system. These are the limited and non-limited version of the revolte joint and the component for the torn body. The combination of modes from these three components forms the modes of the complete system. Figure 5 displays that in total there occur five modes where only two of them are equivalent. Furthermore, there are two intermediate modes for the inelastic impulses that are represented by the vertical lines spanning over the affected components. Here the velocities  $\omega_{R1}$  and  $\omega_{R2}$  are disabled as state variables. Hence, the number of continuous-time state variables in total varies from 2 to 10.

Even for such a simple mechanical system as the trebuchet, it is difficult for a modeler to foresee all of these combinations of modes. In order to enable a truly object-oriented modeling, it is therefore an essential prerequisite that the corresponding simulation environment supports the automatic derivation of these mode combinations and can generate the correct set of equations. If the modeler would be forced to model all modes and their transitions at the top level, the modeling would become extremely laborious. Furthermore, the resulting solution would not be generic, and its parts would hardly be reusable.

### 1.3. Related work

Obviously, the modeling and simulation (M&S) of variable-structure systems is a challenging task. Even a simple mechanical system as the trebuchet poses a number of difficulties for a general M&S framework. Hence, such a system cannot be modeled in Modelica. There are, however, alternative modeling languages that are better geared towards variable-structure systems.

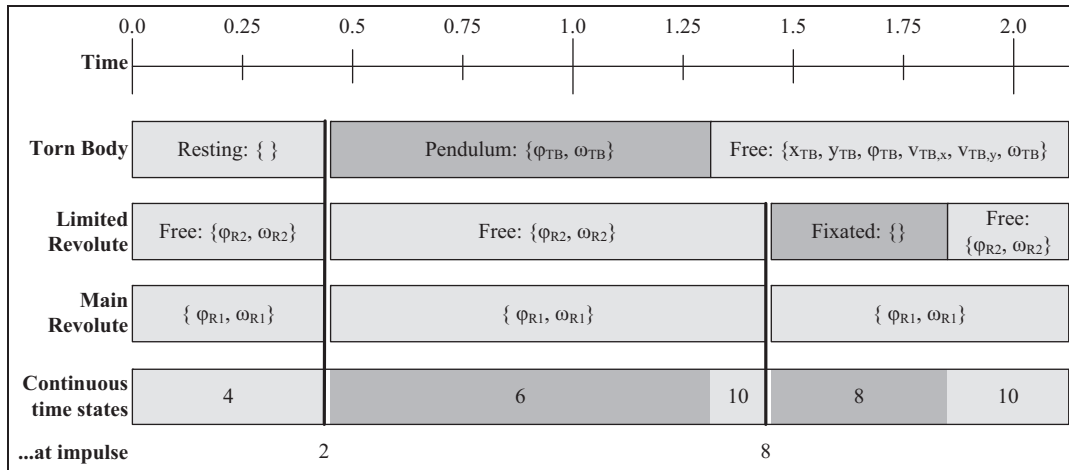


**Figure 5.** Structural changes of the trebuchet.

The project MOSILAB<sup>7</sup> created an extension to the Modelica language that enables the formulation of structural changes by means of state charts. In this way, different parts of the model can be activated or deactivated. To enable a formulation with the aid of state charts, it is necessary that the complete system is decomposable into a finite set of modes. Thus, MOSILAB represents a feasible solution only when the structural changes are modeled on the top level. If, however, these changes emerge from single components, MOSILAB becomes insufficient. The trebuchet represents a suitable example for this. Its implementation in MOSILAB would require that all of its modes are described on a global level. Although theoretical possible, it would be difficult to achieve. The advantage of MOSILAB is that it is a true compiler and generates efficient simulation code.

More promising approaches with respect to a true object-oriented modeling style have been achieved in the field of hybrid bondgraphs. In this methodology, structural changes are modeled by ideal switches that connect or disconnect components of the bondgraph. This suffices for most structural changes in physical systems as long as the number of components is known beforehand. It is insufficient when components need to be instantiated or removed during simulation time. Within the field of hybrid bondgraphs, the projects HYBRSIM<sup>8</sup> and the work of Roychoudhury et al.<sup>9</sup> are notable. In case of HYBRSIM, the bondgraph is simulated by an interpreter that is able to handle up to index-two systems. The work of Roychoudhury et al.<sup>9</sup> favors a translation to a causal block diagram that is being simulated in Matlab Simulink. The approach that tries to preserve the previous causal structure of the bondgraph by applying incremental update algorithms is interesting. It is similar to the approach described in this paper, but less general as it is restricted to bondgraphs.

A recent project is represented by Hydra.<sup>10–12</sup> This is a modeling language that originates from functional programming languages such as Yampa and has been developed at the University of Nottingham. Hydra is based on the paradigm of functional hybrid modeling. This makes it a powerful language. In principle, it is possible to state arbitrary equation systems with Hydra and to formulate arbitrary changes. Also new elements can be generated at run-time. Practically, the simulation engine has not yet been able to demonstrate support higher-index systems to a sufficient extent. The way Hydra is processed is rather unique in the field of M&S. Hydra features a just-in-time compilation. At each structural change, the model is completely recompiled in order to enable a fast evaluation of the system. This approach makes Hydra interesting with respect to this paper since it represents a complementary approach to the incremental algorithms presented here.

Unfortunately, none of these tools demonstrates the ability to model and simulate the trebuchet in a true object-oriented style. Therefore, we decided to develop a new framework called Sol. There are two major objectives behind this project:

1. The language Sol shall enable a true object-oriented modeling style where physical components containing structural changes can be assembled componentwise. This part of the project is published elsewhere.<sup>13–15</sup>
2. The computational framework of Sol shall investigate how the structural changes in the set of DAEs can be handled by incremental algorithms including higher-index problems. To this end, classic methods for index reduction for static systems are revisited and integrated in a more dynamic framework. This is the main content of this paper.



**Figure 6.** Typical processing of equation-based languages.

Hence, we proceed by presenting the computational framework of Sol. Its final capability and performance is then presented in Section 6.

#### 1.4. The Sol framework

Figure 6 depicts the typical processing scheme that is shared by many equation-based languages such as Modelica and involves multiple stages of compilation. It starts with the parsing of the model files and ends with the generation of code that serves simulation or optimization tasks. In this way, a quasi-static computational structure of the model is imposed that prevents the simulation of many classes of structural changes.

In order to enable the handling of variable-structure systems, these processing stages need to be rearranged so that the set of equations can arbitrarily change over run-time. To this end, we provide a new simulation framework called Solsim. Figure 7 depicts the new processing scheme. Since Solsim represents an interpreter, the code-generation is replaced by a direct evaluation. This evaluation stage is used for performing time integration but it may also trigger events that lead to structural changes in succession. To manage these structural changes, new components have to be reinstated and flattened. Furthermore, the causality of the whole system may need to be updated. Thus, these three stages that represented a sequence in the classic processing scheme form now a loop.

The most central part in the processing scheme of Sol is the dynamic DAE processing that replaces the former causalization stage. In this stage, the flattened set of equations is transformed into a set of computations that suits numeric ordinary differential equation (ODE) solvers. It is especially this stage that makes equation-based modeling languages so powerful. The modeler is relieved of the tedious task that consists of the computational realization of his models. It enables also that models can be stated in a declarative manner and are generally applicable. To this end, a great number of elaborate algorithms have been developed for the static case. For many commercial systems such as Dymola<sup>16</sup> most of these algorithms represents the heart of their compiler and partly because of this, their major parts are mostly still under non-disclosure.

Even the static causalization of DAEs is far from being trivial. Handling arbitrary changes in a system of DAEs represents a major challenge. The exchange of single equation may enforce a complete rebuild of the whole computational form. In most of the cases, however, a partial update of the system suffices. In this paper, we present a

framework with its algorithms and methods for the dynamic case that can track changes in an efficient manner.

To this end, it is necessary that we look in detail at the processing of DAEs. Hence, the next four sections present the theoretic fundamentals of the Solsim simulation environment and are not directly application oriented. Section 2 introduces the terminology and presents the basic entities of the applied data structures. Section 3 then explains the handling of index-zero systems and the main principles of our processing algorithm. Systems that contain algebraic loops are discussed in Section 4 whereas higher-index systems are discussed in Section 5. The final section revisits the trebuchet catapult and presents another application example of the Sol framework.

The implementation of Solsim represents a prototype simulator that shall demonstrate the feasibility of the suggested methodology and the functionality of the proposed algorithms. The program itself is a command-line program implemented in C++. The resulting simulation data is dumped to a file. Since the program is a proof of concept and not a mature software tool, the software has not been published but interested readers may contact the author.

## 2. Dynamic DAE processing

### 2.1. Fundamentals

This section defines fundamental notions and terminology used in the following. In order to ease the understanding

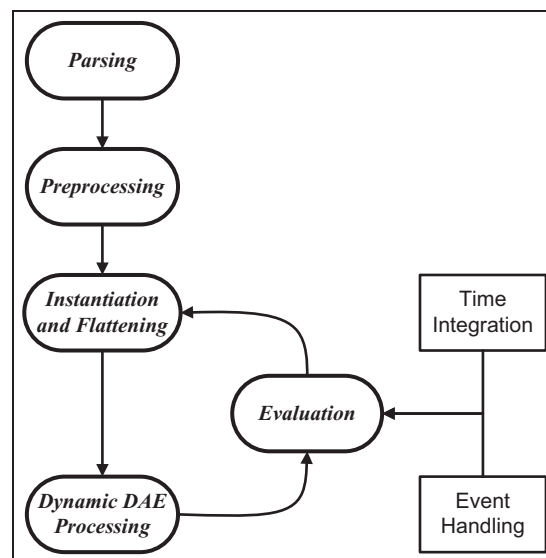


**Figure 7.** Dynamic processing of Sol.

of the abstract definitions, we provide a small and simple example for illustrative purposes. Figure 8 presents an electric circuit with a capacitor. It contains a multi-switch that triggers various structural changes.

Listing 1 presents the corresponding Sol model for this circuit.

---

```

1  model Circuit
2  implementation:
3      static Real R;
4      static Real C;
5      static Real i;
6      static Real u_C;
7      static Real u_R;
8      static Real u_Sw;
9      static Integer mode;
10
11     C = 0.01;
12     R = 100;
13     u_C + u_R + u_Sw = 0;
14     u_R = R*i;
15     i = C*der(x=u_C);
16     mode << f(x=time);
17
18     if mode == 0 then
19         u_Sw = 10;
20     else if mode == 1 then
21         static Real freq;
22         freq = 5;
23         u_Sw = 10*cos(x=freq*(time-5));
24     else if mode == 2 then
25         i = -0.2;
26     else then
27         static Real R2;
28         R2 = 1000;
29         u_Sw = R2*i;
30     end if;
31
32 end Circuit;
```

---

**Listing 1.** Flat Sol model of an electric circuit with multi-switch.

In order to present a concise and traceable example, the Sol model here refrains from any object-oriented constructs that are provided by the language: the model has already been manually flattened and contains no hierarchic structure. The precise syntax and semantics of Sol are outlined by Zimmer.<sup>13</sup> However, the presented example can be briefly explained: it consists of the declaration of variables (e.g. `static Real R;`) and relations. Relations are either non-causal equations (e.g. `u_R = R*i`) or causal assignments. For example, line 15 states that the value of the integer variable `mode` is assigned (with fixed causality) by the result of the function `f` whose input parameter `x` equals time. Please note that the syntax for function calls in Sol (e.g. `f(x = time)`)

requires an explicit binding between formal and actual parameters. Some of the variables and equations are stated within conditional branches (`if ... then ... else ...`). The activation and deactivation of these branches yield structural changes.

The Sol model of Listing 1 represents a set of DAEs. In general, such a system can be described in the implicit DAE form:

$$\mathbf{0} = F(\dot{\mathbf{x}}_p(t), \mathbf{x}_p(t), \mathbf{u}(t), t)$$

The target of the dynamic DAE processor (DDP) is to achieve a transformation of  $F$  into the state space form  $f$  that is directly applicable for the purpose of numerical ODE solution

$$\dot{\mathbf{x}}(t) = f(\mathbf{x}(t), \mathbf{u}(t), t)$$

The level of difficulty of this transformation is described by the perturbation index.<sup>17,18</sup> The transformation itself is consequently denoted as index reduction. This classic DAE perspective is essential but not sufficient. Unfortunately, many models contain more than just DAEs. In particular, variable-structure models are hybrid models that involve both continuous and discrete parts. It is therefore too simplistic to look at the problem from the continuous-time perspective of DAEs only. We need a more general approach.

We give a few remarks regarding the notation of the following sections: lowercase characters are applied to individual entities such as variables, tuples, relations, etc. Capital letters are applied to sets or certain functions.

With respect to relations, when we refer to a specific relation of Listing 1, we use italic line numbers as indices. For instance  $r_{13}$  represents `u_R = R*i`.

**2.1.1. Relations.** We define a system  $s$  as a pair (2-tuple) that consist in a set of active relations  $R$ , a set of active variable identifiers  $V$ :

$$s = (R, V)$$

Mostly, the variables identifiers point to real numbered values, but there are no restrictions applied. The variables identified in  $V$  may be of any basic or compound type. A relation may represent a non-causal equation or a causal assignment of the model. A relation represents typically an equation of the model or a causal assignment. Three functions can be applied on a relation  $r$  in order to determine its dependences on variables in  $V$ .

The system  $s$  often represent just the current mode of the system. For a variable structure system, this means that the sets  $R$  and  $V$  are subject to change during time.

The function  $D(r)$  returns a set of all variables identifiers that the relation  $r$  depends on: its *dependences*. These variables need to be evaluated first before the relation  $r$

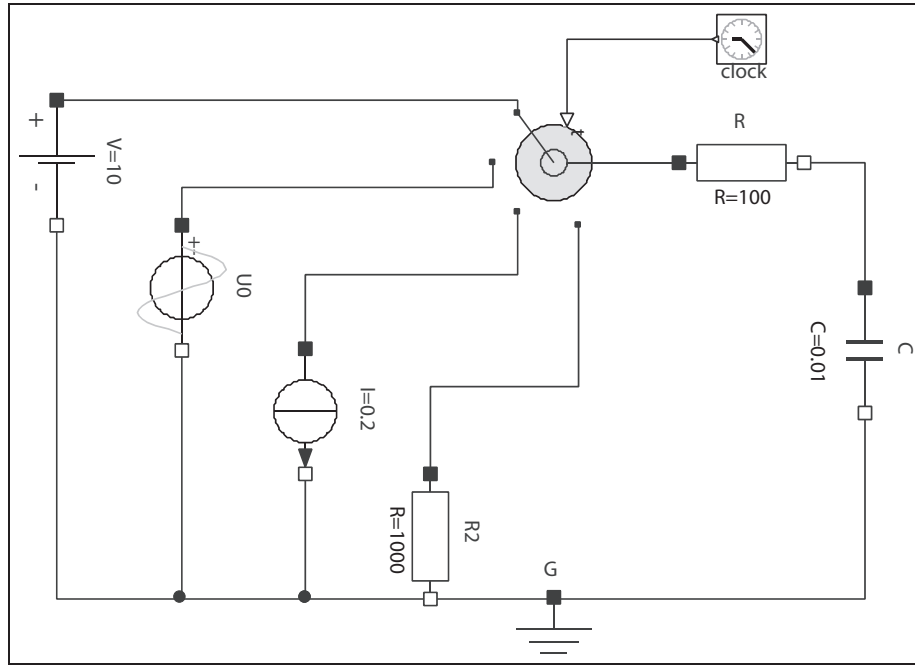


Figure 8. Diagram of an electric circuit with multi-switch.

can be processed. The function  $U(r)$  returns the set of variables identifiers that may be determined by the relation: its *potential unknowns*. Furthermore, the presence in the set  $R$  of a relation may depend on a certain set of variables identifiers that is represented by  $L(r)$ . Such dependences are denoted as *logic dependences*.

For illustration, let us take a look at three relations of our example above.

- $r_{12}$  represents  $u_C + u_R + u_{Sw} = 0$ .

This relation is a simple, non-causal equation between three variables:  $D(r_{12}) = \{u_C, u_R, u_{Sw}\}$ . Since the equation does not stipulate the causality, all of the variables are potential unknowns:  $U(r_{12}) = D(r_{12})$ . There are no logic dependences involved:  $L(r_{12}) = \emptyset$ .

- $r_{15}$  represents  $mode \ll f(x=time)$ .

This relation is a causal assignment and contains two variables of different type:  $D(r_{15}) = \{mode, time\}$ . The assignment predetermines the causality, so there is only one potential unknown:  $U(r_{15}) = \{mode\}$ . Again, there are no logic dependences involved:  $L(r_{15}) = \emptyset$ .

- $r_{17}$  represents  $u_{Sw} = 10$ .

Since this equation is stated within a branch statement, its presence in the active set of relations  $R$  is related to the variable `mode`. This is a logic dependence  $L(r_{17}) =$

$\{mode\}$ . Consequently:  $D(r_{17}) = \{u_{Sw}, mode\}$  and  $U(r_{17}) = D(r_{17}) \setminus L(r_{17})$ .

**2.1.2. Causality graph.** In order to transform the system  $s$  into a form that is useful for computational purposes, we need to assign a causality  $c$  to each of the relations in  $R$ . The causality determines which of the occurring variables an equation should be solved for. Hence, a causality  $c$  is defined to be a pair of a relation and one of its potential unknowns:

$$c = (r, u) \text{ with } u \in U(r)$$

The set of causalities  $C$  has to represent a bijective mapping between subsets of  $V$  and  $R$ . Relations that have a causality assigned are being denoted as causalized, other relations as non-causalized. The sets of variables  $V$ , relations  $R$  and causalities  $C$  can be composed to a tuple:

$$(R, V, C)$$

This tuple can be represented as a causality graph. This is a directed acyclic graph (DAG)  $G(V, E)$  where the vertices represent the relations of the system  $V_G = R$ . A relation  $r_1$  that determines one of its unknowns  $u \in U(r_1)$  has outgoing edges to all of those relations  $r_2$  that are dependent on  $u$ . In this way the causality graph depicts the computational flow:

$$E_G = \{ (r_1, r_2) | r_1 \neq r_2 \wedge ((r_1, u) \in C \wedge u \in D_{r_2}) \}$$

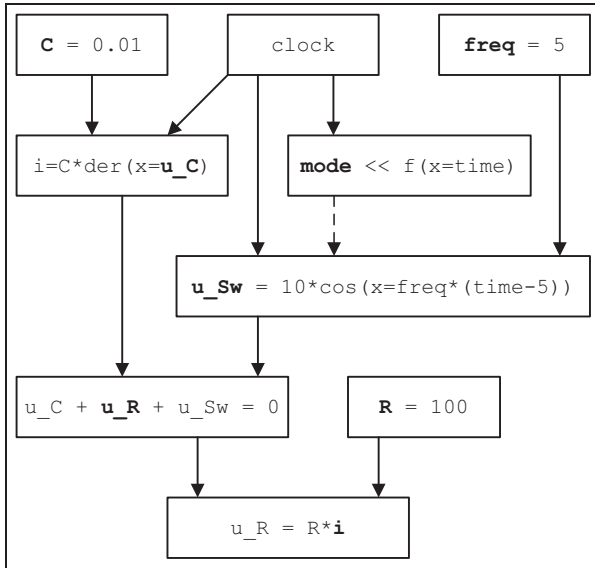


**Figure 9.** Causality graph resulting from Listing 1. The variable that has been selected as the one being determined by a specific relation is highlighted in bold.

In the causality graph, the edges depict the causal dependences within the system of relations. Figure 9 shows a (slightly simplified) causality graph for the example model in `mode == 1`. The relations that include a derivative relation act here as explicit time integrators and depends thus on the (internal) system clock that is stipulating the simulation time. The dashed edge represents a logic dependence in the graph. These dependences assure that relations are not being evaluated before their underlying condition of existence is being checked.

With respect to causality graphs, let us define the following terms. Vertices without ingoing edges are denoted as causal roots. Since a causality graph has to be cycle-free, the terms *predecessor* and *successor* can be defined with respect to any relation  $r$ :

- A relation  $r_a$  is a *predecessor* of  $r_b$  iff there exists a directed path from  $r_a$  to  $r_b$ .
- A relation  $r_a$  is a *successor* of  $r_b$  iff there exists a directed path from  $r_b$  to  $r_a$ .
- *Direct successors* or *direct predecessors* are those relations where the length of the corresponding directed path is exactly 1.

## 2.2. Evaluation within the causality graph

A causality graph can be used to schedule the set of relations into an appropriate order for evaluation. This is always possible, since any acyclic graph gives rise to a partial order on its vertices.

Orderings of the causality graph can also be used for the purpose of code generation instead of a direct evaluation. For instance, a just-in-time compiler can be applied. In this case, one has a strong motivation during a structural change to preserve as much as possible of the causality graph. All parts that remain untouched do not need to be recompiled.

Listing 2 shows one possible schedule that is compatible with the causality graph.

---

<code>C = 0.01;</code>	<code>[C]</code>
<code>i = C*der(x=u_C);</code>	<code>[u_C]</code>
<code>mode &lt;&lt; time &lt; 5;</code>	<code>[mode]</code>
<code>freq = 5;</code>	<code>[freq]</code>
<code>u_Sw = 10*cos(x=freq*(time-5));</code>	<code>[u_Sw]</code>
<code>u_C + u_R + u_Sw = 0;</code>	<code>[u_R]</code>
<code>R = 100;</code>	<code>[R]</code>
<code>u_R = R*i;</code>	<code>[i]</code>

**Listing 2.** A possible schedule resulting from the causality graph. The brackets contain the unknown of each relation.

To attain such a complete order, one can apply a topological sorting algorithm. The standard algorithm<sup>19</sup> works in linear time  $O(|V_G| + |E_G|)$  with respect to the size of the graph. It is however not well suited to cope with the dynamic framework of Sol, since the sorting has to be completely redone whenever the causality graph is changing. Most critical, of course, is the insertion of a new edge. For this purpose, a number of algorithms have been designed that update the ordering by tracking the changes in the graph.

These algorithms are denoted as dynamic topological sorting<sup>20</sup> or on-line topological ordering.<sup>21</sup> Their amortized complexity per edge insertion is in  $O(\sqrt{|E_G|} \log |V_G|)$ . However, a worst-case analysis is misleading since these algorithms perform much better in practice.

## 2.3. The black box

We can abstract the stage of DDP-processing by a specification of its output and input interfaces. The output of the DDP-processing is a causality graph. Furthermore, the output may contain information about over- and underdeterminations of the current system  $s$ .

The input consists in a set of commands that create the desired equation system. The following operations can be applied in order to construct a complete system or to cause a structural change.

- Enter a variable  $v$ :  $V' = V \cup \{v\}$ .
- Enter a relation  $r$ :  $R' = R \cup \{r\}$ .

- Remove a relation  $r$ :  $R' = R \setminus \{r\}$ .
- Remove a variable  $v$ :  $V' = V \setminus \{v\}$ .

This list of operations provides us with an abstraction layer that enables us to interpret the DDP processor as a black box. For convenience, we will use the symmetric difference  $\dot{s}$  between two system  $s_1$  and  $s_2$  to describe a structural change:

$$\dot{s} = \{\dot{R}, \dot{V}\} = (s_1 \setminus s_2) \cup (s_2 \setminus s_1)$$

Hence,  $\dot{R}$  contains all relations that are being removed or added and  $\dot{V}$  contains all variables that are being removed or added.

### 3. Index-zero systems

#### 3.1. Demands on a dynamic framework

In the dynamic framework, variables and their corresponding relations can be added and removed at all times. To avoid overdetermination, old relations are removed from the system before they are replaced by new relations. Thus, intermediate underdetermination must be tolerated. Overdetermination, in contrast, shall be detected immediately.

Both processes, removing and adding, cause changes in the corresponding causality graph. The DDP tracks each of these changes in an efficient manner. However, a worst-case analysis is not a good performance measure, since the replacement of a single relation may cause the recausalization of the whole system. In the worst case, the smartest thing to do is a recausalization of the complete system. Obviously, this is not a good approach in general.

In order to be efficient, the DDP should preserve the existing causality graph as much as possible, so that the causality graph and the corresponding ordering must not be changed more often and more widely than necessary. It is the goal to prevent unnecessary changes in the causality graph and restrict modifications to those parts only that are affected by the change.

#### 3.2. Forward causalization

Forward causalization is the base algorithm for causalization. It assigns a causality  $c$  to a non-causalized relation  $r$ . It represents a simple straightforward algorithm, a variant of topological sorting that is part of many similar algorithms, for instance the Tarjan algorithm.<sup>22</sup>

This algorithm can be implemented as a graph algorithm. In the dynamic framework, this procedure is executed whenever a new relation is added. It calls itself recursively and potentially updates all successors of the relation. For Algorithm 1 and all following algorithms, the sets  $R$  (relations),  $V$  (variables), and  $C$  (causalizations) are available as global variables.

---

**Input:** a relation  $r$

**Output:** causality  $c = (u, r)$

$D'$  is the set of direct predecessors of  $r$ .

It is initially empty:  $D' := \emptyset$ ;

**for** all  $v \in D(r)$  **do**

**if**  $v$  is determined,

        i.e.  $(v, r') \in C$  with  $r' \neq r$  **then**

$D' := D' \cup \{v\}$ ;

**end**

**end**

Attempt to causalize  $r$ , given  $D'$ ;

**if** causalization was successful **then**

    Retrieve its unknown  $u$ ;

    Assign and enter the causality:  $C := C \cup \{(u, r)\}$ ;

**for** all relations  $r_a$  succeeding  $r$  with  $u \in D(r)$  **do**

        apply forward causaliz. recursively for  $r = r_a$ ;

**end**

**end**

---

**Algorithm 1.** Forward causalization.

The actual causalization of a single relation  $r$  is not described here, but later on in Section 3.6. However, the causalization of  $r$  depends always on its knowns  $D' \subseteq D(r)$  and on its kind. There are two kinds of relations in Sol: causal relations (assignments) and non-causal relations (equations).

For instance, a causality can be assigned for non-causal relations, if all but one element of  $D(r) \setminus L(r)$  are determined by other relations. Further kinds of relations are presented in Sections 4 and 5 that have their own characteristics and serve special purposes.

If the computational flow of a system can be expressed in the form of a simple causality graph, forward causalization is fully sufficient. Forward causalization will fail, if the system is under- or overdetermined. It will fail as well, if the system contains algebraic loops. This case is discussed in Section 4.

Another reason for failure is that not all relations can be solved for all of its unknowns. For instance, a relation  $r$  like  $\sin(x=\text{phi}) = a$  can only be solved for  $a$  but not for  $\text{phi}$ . However, this demands no modification of the presented algorithms. The inability to solve for  $\text{phi}$  is simply expressed by the set of unknowns:  $U(r) = \{a\}$  whereas  $D(r) = \{a, \text{phi}\}$ . If the causal structure of the system demands for instance the inversion of the sine function, an artificial algebraic loop will result by the application of the methods in Section 4.

#### 3.3. Potential causality

The reverse process to forward causalization would be forward decausalization. It consists in removals of causalities in  $C$ . One could implement this in a similar way. This process would then be executed, each time a relation is removed. However, this represents an overeager approach, since each

structural change might involve a temporal underdetermination of the system. If this temporal underdetermination affects a causal root of the system, forward decausalization would remove many or even all causalities from the system, just to see them potentially reinstated a few steps later.

In order to avoid such overhasty reconfigurations of the causality graph, we introduce the concept of *potential causalization*. This means that, once a causalization has been assigned to a relation, the relation will not lose this causality again. This is even the case if some of its “knowns” are not determined anymore; instead the relation is being marked as potentially causalized.

Whenever a relation  $r$  with its causality  $c(u, r)$  is removed, the following steps are executed:

1. The causality  $c = (u, r)$  is removed:  $C := C \setminus \{(u, r)\}$ .
2. Attempt to causalize all direct successors  $r_{succ}$  of  $r$ .
3. If the attempt fails, the relation  $r_{succ}$  remains *potentially causalized*.
4. Remove  $r$ :  $R := R \setminus \{r\}$ .

For instance, let us consider the switch from mode 1 to mode 0 in the example of Listing 1:  $\dot{s} = (\{r_{17}, r_{20}, r_{21}\}, \{\text{freq}\})$ . First, the two relations  $r_{20}$  and  $r_{21}$  are removed. The relation  $r_{12}$ , representing  $u_C + u_R + u_{Sw} = 0$  is dependent on  $r_{21}$  and is therefore causalized again. It remains potentially causalized.

Now the relation  $r_{17}$  is added to the system. It is directly causalized by the subsequent forward causalization and determines  $u_{Sw}$  again. As a consequence,  $r_{12}$  releases its potential state, and the causality graph is once more complete. This specific structural change could be handled with minimal effort: no unnecessary decausalization had to be performed.

### 3.4. Causality conflicts and residuals

Potentially causalized relations only replace their former causality, if they are being contradicted by other relations. To illustrate this, let us suppose that we are now switching from mode 0 to mode 2 in the example model. The corresponding change is  $\dot{s} = (\{r_{17}, r_{23}\}, \emptyset)$ .

This change does yield a causality conflict. After removing the relation  $r_{17}$ ,  $r_{12}$  remains potentially causalized. The newly added relation  $r_{23}$  cannot be causalized, since its only potential unknown  $i$  is already determined by the relations  $r_{13}$ , representing  $u_R = R \cdot i$ . The relation  $r_{23}$  is overdetermined.

To cope with this conflict,  $r_{23}$  generates a residual  $\rho$  and  $U(r_{23})$  expands in correspondence. The residual  $\rho$  represents the difference between the two sides of the equation. It should of course be zero. Also the causality  $c = (\rho, r_{23})$  is generated. Residuals are globally collected in the set  $\Omega$ . Whenever the process of forward causalization stops and  $\Omega \neq \emptyset$ , the residuals are *thrown*. Throwing residuals means that sources of overdetermination are looked up and assigned to the residual. Potentially causalized relations represent one possible source of overdetermination.

The lookup for sources includes all predecessors of the relations that determine a residual. Whenever a potentially causalized relation is assigned to a residual, all causalities of the corresponding predecessor paths are first marked and finally collectively removed. Algorithm 2 presents one possible implementation. It detects all sources in a recursive depth-first traversal and marks them and all of their predecessors while tracking back the traversal path. Finally all marked relations are decausalized.

In the given example, the relation  $r_{12}$  is potentially causalized and assigned to the residual as source of overdetermination. The relations  $r_{13}, r_{23}$  are those predecessors of the residual that are successors of  $r_{12}$  and are marked by adding them to the set  $P$ . Their causalization is collectively removed.

By applying forward causalization on the members of  $P$ , the relation  $r_{23}$  will be causalized again and remove its residual, since it determines the variable  $i$ . The conflict has been resolved, and all relations can be causalized. In general, the lookup for the potential path can be achieved by the recursive Algorithm 2. The algorithm is called for the relations that have thrown the residuals in  $\Omega$ .

The presented processing scheme represents the general approach of the DDP.

1. Overdetermined relations generate a residual. This residual is *thrown* into the set  $\Omega$ .
2. When forward causalization stops, all residuals in  $\Omega$  are examined.
3. The examination looks for a source of overdetermination in all predecessors of the corresponding overdetermined relation.
4. If a source is found, the conflict is resolved by means appropriate to the type of the source.

---

**Input:** a relation  $r$

**Output:** global set  $P$  of members of the potential path  
Initially (non-recursive),  $P := \emptyset$ ;

Recursive section:

```

for each direct predecessors  $r_a$  of  $r$  do
  if  $r_a$  is potentially causalized then
     $P := P \cup \{r, r_a\}$ ;
  else
    call this algorithm recursively for  $r = r_a$ ;
    if  $r_a \in P$  then
       $P := P \cup \{r\}$ ;
    end
  end
end

```

**end**

Finally (non-recursive) **begin**

```

for each  $r' \in P$  do
  remove causality:  $C := C \setminus \{(-, r')\}$ ;
end
for each (non-causalized)  $r' \in P$  do
  perform forward causalization on  $r'$ ;
end

```

**end**

---

**Algorithm 2:** Potential path detection and removal.

The last point in the list makes a very general statement: “by means appropriate”. For this particular problem, overdetermination was caused by potentially causalized relations. The appropriate procedure was to recausalize the path that has been potentially causalized.

We shall see in the next sections that there are other sources of overdetermination as well. They will call for other means in order to resolve the conflict, but the outlined processing scheme proves to be of general value.

### 3.5 Avoiding cyclic subgraphs

The causality graph is defined to be an acyclic graph. If it is constructed solely by the process of forward causalization, it is guaranteed to be acyclic. Yet having potentially causalized relations in the graph, this statement does not hold true anymore. We need to ensure that it remains acyclic.

A cycle may occur whenever a potentially causalized relation  $r_p$  gets causalized again. If this occurs, one has to verify that none of the predecessors of  $r_p$  is also a successor of  $r_p$ .

If the verification fails, the graph contains a *cyclic subgraph* with at least one potentially causalized relation. The cyclic subgraph is defined to be the union of all directed paths starting and ending at  $r_p$ . The causalities of all relations belonging to this cyclic subgraph have to be removed. An algorithm for this purpose would be similar to Algorithm 2.

Their causality will not necessarily get reinstated by further forward causalization. The system may contain an algebraic loop. An example for this is the switch from mode 0 to mode 3 with  $\dot{s} = (\{r_{17}, r_{26}, r_{27}\}, \{R2\})$ . Again  $r_{12}$  becomes potentially causalized. After adding  $r_{26}$  the relation  $r_{27}$  is added and is causalized to  $u\_Sw$ . This would reinstate the causality of  $r_{12}$ , but  $r_{12}$ ,  $r_{13}$ , and  $r_{27}$  form a cyclic subgraph. All their causalities will be removed.

Forward causalization will not be able to complete the causalization anymore. However, the system is not underdetermined. It contains an algebraic loop. For this particular example, this means that a linear equation system needs to be solved, in order to compute the voltage divider that is created by the two series-connected resistors. Section 4 will discuss how such systems and more complicated ones can be handled in a dynamic manner.

### 3.6. States of relations

We have not yet described how the causalization of a single relation works. We know from the previous sections that the dynamic framework expects that the relations can be in different states. By name, these are:

- *non-causalized*: the relation has no causality  $c$  assigned to it;
- *potentially causalized*: the relation retains its former causality although it is currently not valid anymore;
- *causalized*: the relation determines one of its potential unknowns;
- *causalized with residual*: the relation is overdetermined and determines a residual.

The dynamic framework may remove the causality of any relation at any time, as this happens with the potentially causalized paths that lead to a residual. Otherwise, the relation may change its state by any attempt of causalization during forward causalization.

The transition between the states is best described by a state-transition diagram. It is dependent on the type of the relation. Sol offers mainly two types: equations, these are non-causal relations; and transmissions, these are causal relations.

For instance, equations in Sol represent non-causal relations  $r$  and fulfill the condition  $U(r) = D(r) \setminus L(r)$ . In order to be causalized, they require that all but one variable of  $U(r)$  are causalized. Figure 10 depicts the corresponding behavior of non-causal relations. The labels at the edges denote the events that trigger a state transition. If none of these conditions is fulfilled, the relation rests in its current state. The states *not-causalized* and *causalized* may serve as intermediate states.

### 3.7. Asymptotic complexity

The first objective is to show that the proposed algorithms terminate. The second objective is to present an upper bound for the complexity of the algorithms. Since these algorithms are graph algorithms, it is the most natural choice to use the number of vertices  $|V_G|$  and the number of edges  $|E_G|$  as definition for the problem size. Often however, one is simply referring to the system size  $n$ . For all meaningful applications of Sol, it is a safe assumption to state that  $n = |V_G|$  and  $O(|E_G|) = O(|V_G|)$ . The latter assumption implies the sparsity of the equation system.

Let us start with forward causalization. This algorithm will terminate simply because it can only increase the number of variables that are being determined by a relation. This requires that the individual relations do not lose their causality by the determination of arbitrary variables. This requirement is fulfilled for both kinds of relations.

The causality graph is generated by forward causalization. The state transitions for causal and non-causal relations imply that a relation can be causalized if it is a causal root or if all of its predecessors in the causality graph have been causalized. Since forward causalization will process all relations at least once, all causal roots will

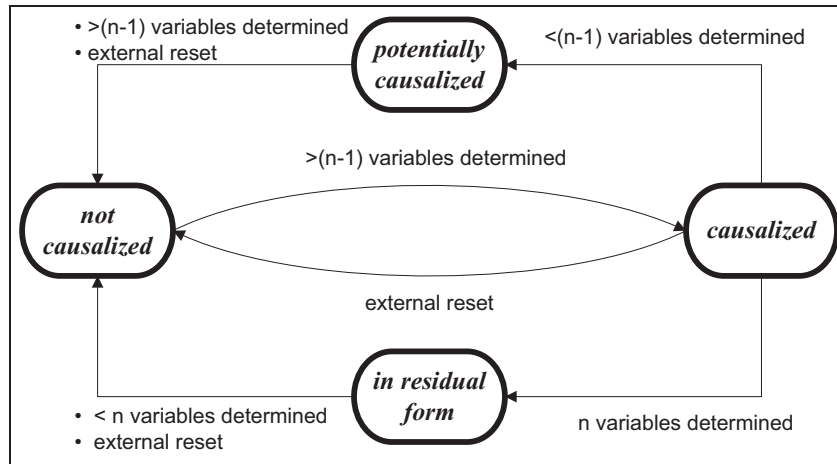


**Figure 10.** State transitions of non-causal relations. The cardinality of  $U(r)$  is denoted as  $n$ .

be causalized. Since the algorithm processes all direct successors of a causalized relation, also the non-root relations will be causalized. Forward causalization fails if there are algebraic loops or equations that cannot be causalized as desired because of non-linearities.

The algorithmic complexity of forward causalization is, not surprisingly, the same as for the topological ordering. Each relation is processed at least once. If a relation has been causalized, all its outgoing edges are being traversed. If all relations have been causalized, all edges will have been traversed. Since each relation is causalized only once, the total complexity of the algorithm is in  $O(|V_G| + |E_G|)$  or  $O(n)$ .

Here  $O(|V_G| + |E_G|)$  is also the upper bound for any traversal of successors or predecessors in the causality graph. Hence, the throwing of residuals requires  $O(|\Omega|(|V_G| + |E_G|))$ , since each residual requires a traversal of its predecessors in order to find its sources of overdetermination. It is possible to reduce the upper bound to  $O(|V_G| + |E_G|)$  by a collective traversal in the graph, but that does require an additional, non-constant cost in memory per vertex in the graph.

Another traversal of successors or predecessors is needed to assure that the causality graph remains cycle free. Hence, the recausalization of potentially causalized equations requires costs in  $O(|V_G| + |E_G|)$ . Mostly, however, this operation is much cheaper. The ordering that is required for the evaluation of the causality graph may be used for a quick test if the graph is cycle-free. In our implementation, we use priority numbers, and in this way, cycle-freeness can be quickly affirmed.

Finally, we have to show that any arbitrary structural change is handled correctly. Since such a change may cause an alternating sequence of forward causalizations and causality removals, it is not evident that the algorithm will terminate. Therefore, it is of importance that all residuals are collectively thrown and the corresponding

potential paths are collectively removed. This includes the potential cycles.

By doing so, one ensures that the subsequent forward causalization is processed on a subgraph without potentially causalized relations. If there remain residuals or new residuals have been created, there will be no source of overdetermination for them, and the residuals indicate an overdetermination of the complete system.

In this way, four steps are sufficient to correctly handle any structural change that leads to a regular system of index-zero.

1. Equations that are being replaced are removed. Their direct successors remain potentially causalized.
2. New equations are added to the system. Forward causalization is applied to them. Potential causalizations may get re-established.
3. Residuals are thrown (if any). Potentially causalized paths are reset.
4. Forward causalization is executed once more on the reset part.

It is possible to implement all these steps in  $O(|V_G| + |E_G|)$ . This guarantees that the handling of structural changes has the same algorithmic complexity as a complete rebuild of the system. This would be optimal since the worst-case scenario would cause a complete rebuild. The following list describes those structural changes in index-zero systems that can be handled more efficiently.

- Structural changes that add components to the existing computational flow.
- Structural changes that replace components but retain the computational flow.
- Arbitrary structural changes that depend only on a small set of variables.

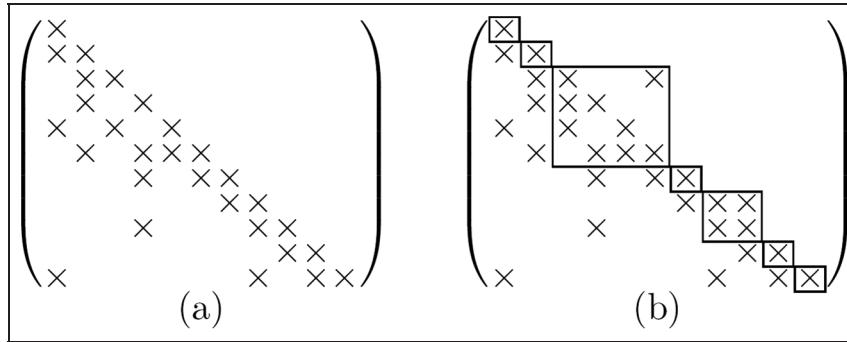


Figure 11. Two structural incidence matrices: (a) in lower-triangular form; (b) in BLT form.

## 4. Index-one systems

### 4.1. Algebraic loops

The target of the DDP is to transform the system  $s = (R, V)$  of relations into a form that is suited for numerical evaluation. To this end, the evaluation stage and the DDP share the same data structure: a causality graph.

Nevertheless, let us look at another representation of the system  $s$ : the so-called structure incidence matrix.<sup>23,24</sup> This is a Boolean matrix  $M$ , where the rows correspond to the relations  $R$ , and the columns refer to the variables  $V$ . The order of rows and columns is given by  $p_V$  and  $p_R$  that assign to each integer of the index range an element of the corresponding sets  $V$  and  $R$ . The values  $M(i, j)$  of the matrix are then defined by

$$M(i, j) = (p_V(i) \in p_R(j))$$

Since the causality graph gives rise to a partial order of its relations, it can be used to directly determine  $p_V$  and  $p_R$  such that  $M_s$  has a lower triangular form where the unknown of each relation is placed on the diagonal. Figure 11(a) depicts an example of such a matrix. This form is highly desired, since it enables the direct solution of the whole system through forward substitution. Unfortunately, it cannot not be achieved for all DAEs.

The most desired form that can represent all possible index-one systems of equations is the block lower triangular (BLT) form.<sup>25</sup> Here the system is divided into lower triangular parts and blocks. An example is depicted in Figure 11(b). It contains two diagonal blocks, one of size 4 and one of size 2. They are separated by a lower triangular part of size 1. In order to transform a system into BLT form with minimal block sizes, one can apply the Dulmage–Mendelsohn permutation,<sup>26</sup> whose central part consists in the strong component analysis of Tarjan.<sup>22</sup> The BLT transformation is efficient since the Tarjan algorithm has a complexity of  $O(|V_G| + |E_G|)$ . The blocks in the matrix

represent these strong components. We denote them also as algebraic loops.

The term *perturbation index*<sup>17,27</sup> formalizes the difference between systems that are directly solvable through forward substitution and those that require at least subsystems of equations to be solved. Index-zero DAEs are directly transformable into ODE form. DAEs that contain one or more algebraic loops are of at least index one.

Because algebraic loops originate from the object-oriented models, they are mostly inflated. This means that they include a significant number of intermediate or auxiliary variables that result out of the object-oriented formulation of the model. Hence, the corresponding blocks are mostly sparse, and a few variables are often sufficient to determine the complete subsystems. The preferred method is therefore often the *tearing* method.<sup>23,28</sup> To this end, we determine a sufficient number of tearing variables and assume them to be known. The forward causalization of the block is now possible and will generate overdetermined equations that yield residuals. The number of residuals will match the number of tearing variables, if the subsystem is regular. Given the pair of the tearing vector and its corresponding residual vector, it is now possible to solve the system by any iterative solver, as for instance Newton's method or the secant method.

The procedures outlined so far represent a common approach for the static treatment of DAEs. They are however insufficient for a dynamic framework, such as Sol. The methods and algorithms of the DDP differ therefore from the outlined procedure. For instance, it is not efficient to acquire a BLT transformation after every structural change, especially considering the fact that intermediate underdeterminations shall be tolerated. For this reason, we refrain from finding the strong components in advance and will identify them at a later stage by an analysis of the resulting residuals.

The following sections will explain the methodology of the DDP. These explanations are supported by a small example in Listing 3.

---

```

1  model Circuit2
2  implementation:
3    //declarations are omitted    [...]
4    u1 = 10*sin(time*pi*50);
5    u2 = 5*sin(time*pi*30+pi/4);
6    u3 = 16*sin(time*pi*20+pi/2);
7    u1-v1 = R1*i1;
8    u1-v2 = R12*i12;
9    u2-v2 = R2*i2;
10   u3-v2 = R23*i23;
11   u3-v3 = R3*i3;
12   v3-v2 = R5*i3;
13   i1 + i12 + i2 + i23 + i3 = 0;
14   cout << v1 + v2 + v3;
15
16   static Boolean closed;
17   closed << f(x=time);
18
19   if closed then
20     v1 - v2 = R4*i1;
21   else then
22     i1 = 0;
23   end if;
24 end Circuit2;

```

---

**Listing 3.** Flat Sol model of a resistor network.

It represents an electric circuit (cf. Figure 12) that linearly combines three voltage sources through a resistor network.

To illustrate the algebraic loop, let us suppose that the switch in the circuit is open: so the equation  $r_{20}$  holds. The process of forward causalization will then manage to causalize the relations  $r_4, r_5, r_6, r_7, r_{16}, r_{20}$  and determine the variables  $u_1, u_2, u_3, v_1, \text{closed}, i_1$ . The rest of the systems represents an algebraic loop.

An algebraic loop cannot be directly represented in a causality graph because the graph would contain a strong component<sup>24</sup> and the graph would not be acyclic. Forward casualization generates only acyclic graphs and hence will fail for systems that contain algebraic loops.

**4.1.1. Example tearing.** In order to complete the causalization of the example system, we can proceed by applying the tearing method. First, we have to choose a tearing variable. Let this for instance be  $v_2$ . Further we state that this variable is now determined. This assumption will enable the forward causalization of the relations  $r_8, r_9$ , and  $r_{10}$ . Furthermore, relations  $r_{11}$  and  $r_{13}$  are being causalized.

The equation  $r_{12}$  is now overdetermined and therefore transformed into residual form:  $\rho = (v_3 - v_2) - (R_5 * i_3)$ . This residual may then be used as a target for root-finding algorithms. Since all equations of the loop are linear in this example, a single Newton iteration on the tearing variables would be sufficient.

**4.1.2. Representation in the causality graph.** In the causality graph, we cannot directly represent algebraic loops but we can represent the torn loops. To this end, we introduce a new kind of relations: the *tearing relation*. It forms an additional node in the causality graph that expresses the selection of the tearing variables.

A tearing relation may be added by the system in order to determine an arbitrary vector of variables. In return, the resulting vector of residuals is managed by a special residual relation. In contrast to normal types of relations, these special relations may determine several variables.

The causality graph of our example model (with an open switch) is depicted in Figure 13. The torn loop forms a subgraph, and hence all of its members are grouped by a frame. The root within this frame is the tearing relation. Although it is solely determined by the simulation system and its (iterative) solvers, the tearing relation is made dependent on all of those relations outside the loop that determine any variables used inside the loop. In this way, any premature evaluation of the loop is avoided.

The sink of the algebraic loop is the residual relation. All relations outside the loop that use variables determined within the loop are made dependent on the residual relation. In this way, their premature evaluation is prevented.

## 4.2. Selection of tearing variables

The predominant procedure in the DDP processing is forward causalization. Whenever algebraic loops occur, forward causalization will stop and leave the remaining part non-causalized. This remaining part may now consist of several blocks of different sizes. However a complete BLT transformation is not desired in an incremental framework and, thus, the selection of tearing variables takes place without knowing the individual blocks.

Whenever a tearing variable has been selected, forward causalization is executed again, and an increasingly larger part of the system gets causalized. Selection of tearing variables and forward causalization may therefore be executed alternately several times, until the complete system has been causalized.

The effort that is needed for the evaluation of an algebraic loop is dependent on the selection of tearing variables, and different selections may yield different residuals. Let us suppose we have chosen the variables  $i_{23}$  and  $i_3$  instead of  $v_2$ . Then two residuals would result, for instance out of  $r_{12}$  and  $r_{13}$ . We shall later see that the former residual is a fake residual (cf. Section 4.4) that reveals  $i_3$  as an obsolete tearing variable. Although the choice of tearing variables is arbitrary, there are good choices and bad ones.

In general, the solution of a linear or non-linear equation system requires an effort that is cubic to the size of the residual vector.<sup>29</sup> Hence, we would like to choose the

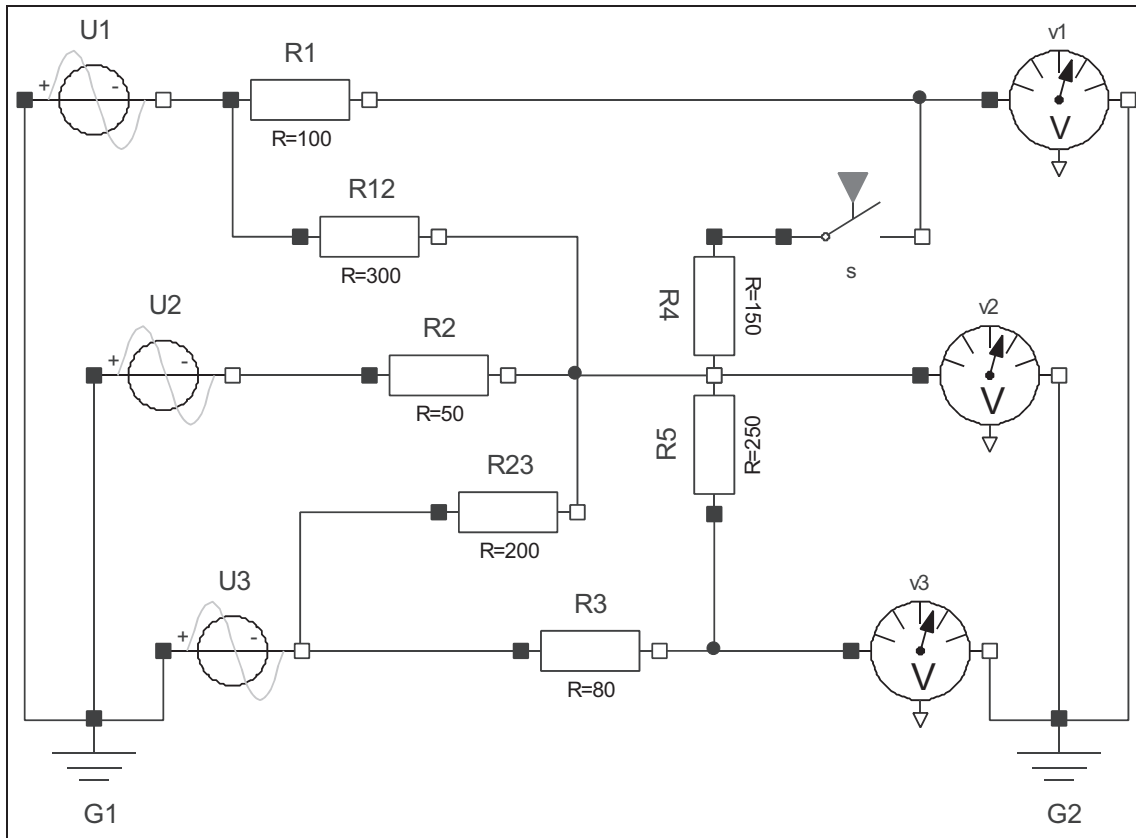


**Figure 12.** Electric circuit diagram of a resistor network.

tearing variables such that a low number of preferably small residual vectors result. This would optimize the following term:

$$\sum_i^{N_\rho} |\rho_i|^3$$

where  $\rho_i$  represents a residual vector, and  $N_\rho$  represents their total number. Unfortunately, this is presumed to be an NP-hard optimization problem.<sup>28</sup> A standard depth-first search for the optimal set of tearing variables will therefore need exponential time. In a first approach,<sup>25</sup> a reduction of the problem was suggested using a so-called cycle matrix. This algorithm will find the best tearing, but even the reduction to the cycle matrix needs exponential time (at least as proposed by Steward<sup>25</sup>). Other approaches use dynamic programming but require even an exponential amount of memory.<sup>30</sup>

Also non-optimal tearing variables can be used, and hence some algorithms attempt an approximation. The algorithm of Ollero and Amselem<sup>31</sup> tries to deduce a good tearing by contracting equations and eliminating variables in alternation. The algorithm proceeds in polynomial time, but an analysis of the output performance for this algorithm is missing.

Many processors of DAEs (as Dymola) are based on or supported by heuristics. One possible heuristic is proposed by Cellier and Kofman,<sup>23</sup> but also this set of rules may lead to arbitrarily bad performance.

Nevertheless in a dynamic framework, expensive optimization algorithms are mostly not affordable, and we restrict ourselves to a rather simple heuristic approach. Since it is the goal of the tearing to enable a subsequent forward causalization, it seems a natural choice to take any variable out of the equation that is the closest to being causalized. This will be the equation that contains the smallest number of undetermined variables. We can refine this heuristic by choosing the variable out of these equations that is shared by the most other non-causalized equations and is therefore likely to cause further forward causalizations.

It is important to note that the optimality of a tearing has been solely regarded from a structural viewpoint. Even if the torn system is structurally regular, it might still be numerically singular or ill-conditioned. With respect to the numerical evaluation, a small set of tearing variables is definitely preferable but not the only aspect. In particular, for non-linear systems, it may occur that a larger set of tearings can lead to a numerically better solution.

Unfortunately, these numerical considerations are hard to quantify and to relate with the structural criteria. Within

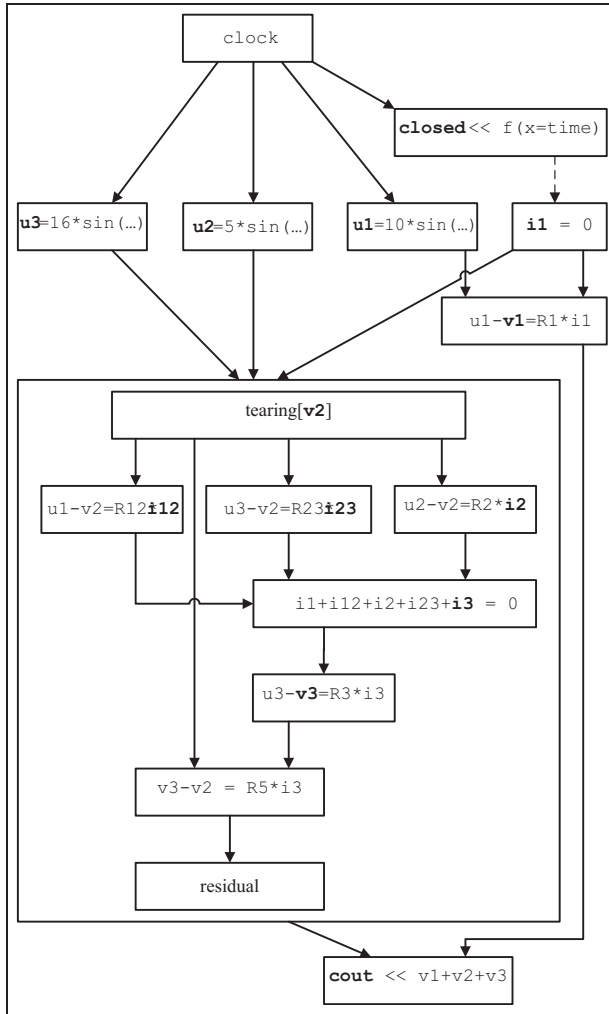


Figure 13. Causality graph with a torn algebraic loop.

the framework of Sol, these aspects are only taken into account in a limited way.

For certain relations in Sol, the set of potential unknowns  $U_r$  is artificially restricted. This may be the case for non-linear equations such as  $a = \sin(x=b)$  or for linear equations that involve a potential division by zero such as  $a = b \cdot C$  with  $C$  being a variable. This restriction reduces the set of possible causalizations and may give rise to additional tearing variables or even complete algebraic loops that would not be required from a purely structural viewpoint.

#### 4.3. Matching residuals

As described in the previous section, forward causalization will detect overdetermined equations and generate corresponding residuals. Those are collected in the set  $\Omega$ . In a second stage, those residuals are thrown. This means that we investigate their predecessors for potential sources of

overdetermination. Tearing relations are one possible source of overdetermination.

In order to extract the algebraic loops, we need to match the residuals to their corresponding tearing variables. The members of the algebraic loop are finally determined by a pair consisting in a vector of tearing variables and its vector of residuals. A complete system may contain several loops and, hence, several pairs. To find the optimal decomposition into pairs is not a trivial task.

Again, a graph representation helps further analysis. The set of tearing variables  $T$  and the set of residuals  $\Omega$  form vertices of a bipartite graph  $G_B((T, \Omega), E_B)$  where the edges  $E_B$  represent the set

$$E_B = \{(\tau, \rho) \mid \tau \in T \wedge \rho \in \Omega \wedge \tau \text{ is predecessor of } \rho\}$$

In order to form a pair that consists of a tearing vector and a residual vector, we have to find the smallest subset of residuals  $\Omega_T \subset \Omega$ , so that the size of its direct neighbors  $\delta$  (that are in  $T$ ) is equivalent:  $|\Omega_T| = |\delta(\Omega_T)|$ .

For arbitrary bipartite graphs, this is a difficult optimization problem. For regular systems of equations that contain no singularity, the number of residuals must match the number of tearing variables. Here we can derive an optimal decomposition in polynomial time. The first objective is therefore to extract a component from the bipartite graph so that both partitions are of equal size. We shall use the greedy Algorithm 3 for this purpose.

---

```

T' := ∅;
Ω' := ∅;
repeat
  Ω̃ := Ω \ Ω';
  select ρ ∈ Ω̃ with smallest neighborhood δ(ρ) in T \ T';
  Ω' := Ω' ∪ {ρ};
  T' := T' ∪ δ(ρ);
until Ω̃ = ∅ or |T'| = |Ω'|;
if |T'| = |Ω'| then
  found one matching: (Ω', T');
  restart algorithm to find another matching for:
  Ω := Ω \ Ω';
  T := T \ T';
else
  no matching could be found;
end

```

---

Algorithm 3. Greedy matching algorithm for residuals.

For each component in  $G_B$ , we start with the residual  $\rho_1$  that owns the smallest neighborhood  $\delta(\rho_1)$  and store it in the set  $T'$ . The residual is stored in  $\Omega_{T'}$ .  $T'$  shall be larger than  $\Omega_{T'}$ , otherwise we have an overdetermined system (see Section 4.7.1). The next residual  $\rho_2$  shall be the one in the neighborhood of  $T'$  so that  $\delta(\rho_2) \setminus T'$  is minimal.

Whenever  $\Omega_{T'}$  becomes equivalent in size to  $T'$ , we have found a pair and can close the tearing. Thereby the sets  $T'$

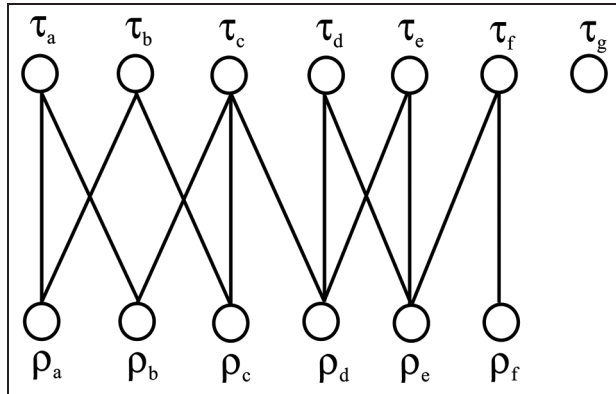


**Figure 14.** A bipartite graph that is used to match residuals to their corresponding tearings.

and  $\Omega'_T$  are removed from the graph, and we can continue with the algorithm for the remaining graph.

Figure 14 presents a small example (that is not correlated with the prior examples): the graph consists of two components. The small component that is just the node  $\tau_g$  represents a tearing with no matching residual. There is no loop that can be closed yet. Further tearing variables will have to be selected in order to causalize the remaining parts of the system and yield the required residuals. Alternatively, the system could turn out to be underdetermined.

Let us focus on the large component. We select  $\Omega' = \{\rho_f\}$ . The neighborhood  $T' = \{\tau_f\}$  is then of equal size and we can close this loop:  $\rho_f$  and  $\tau_f$  form a pair and are both removed from their global sets  $\Omega$  and  $T$ . We restart the algorithm for the remaining part of the bipartite graph:

1.  $\Omega' = \{\rho_a\} \Rightarrow T' = \{\tau_a, \tau_b\}$ ;
2.  $\Omega' = \{\rho_a, \rho_b\} \Rightarrow T' = \{\tau_a, \tau_b, \tau_c\}$ ;
3.  $\Omega' = \{\rho_a, \rho_b, \rho_c\} \Rightarrow T' = \{\tau_a, \tau_b, \tau_c\}$ .

After three steps, we have found another matching pair of a tearing vector  $(\tau_a, \tau_b, \tau_c)$  and a residual vector  $(\rho_a, \rho_b, \rho_c)$ . There remain two residuals  $(\tau_d, \tau_e)$  with two corresponding tearing variables  $(\rho_d, \rho_e)$ . At the end, there are three tearings that could be closed. In this example, the greedy algorithm led to the optimal solution, but if we would have chosen  $\rho_e$  in place of  $\rho_a$ , the outcome would have been different: the last two resulting tearings merge to one tearing of size five. This outcome is not optimal anymore. The proposed greedy algorithm is not even an approximation algorithm. Counterexamples can be provided that lead to an arbitrarily bad performance of the result.

To derive the optimal decomposition in polynomial time, we have to assume that the system is regular. This assumption holds true for the result of the greedy algorithm (Figure 15(a)). For a regular system, it must be possible to

assign each tearing to a residual. Hence, the bipartite graph contains a perfect matching.<sup>24</sup> This is a maximum matching covering all vertices. It can be found in a bipartite graph within  $O(\sqrt{|(T, \Omega)|}|E_B|)$ .<sup>19</sup> Once the perfect matching has been found, we turn all of those edges that do not belong to the matching into directed edges pointing to the residuals (Figure 15(b)).

If we now join the vertices that share an edge of the perfect matching, there results a directed graph (Figure 15(c)). The strong components of this graph now indicate the optimal decomposition. If a tearing with its matched residual is not strongly connected to another one, this means that the corresponding systems of equations can be solved separately. As shown before, the strong components can be extracted by the Tarjan algorithm in  $O(|T|^2)$  where  $|T|^2$  is an upper bound for the maximum number of edges. Essentially, this procedure represents the approach of the Dulmage–Mendelson permutation,<sup>26</sup> simply performed on an extracted subset of tearing variables and residuals instead of the whole system of equations.

In this way, we can avoid a strong component analysis for the complete system of relations and instead perform the analysis on the set of tearings and residuals. Here, the problem size is (for all problems of interest) much smaller, and the blocks of the BLT form can be derived after the causalization has taken place. Since the tearings are also more robust with respect to a temporary underdetermination, this approach suits the demands of a dynamic framework much better and justifies the blind tearing without a priori knowledge of the BLT form.

Finally, an algebraic loop is represented by a diagonal block in the structure incidence matrix. Knowing a pair of tearing and residual vectors enables us to extract such a block from the system. We denote the corresponding process as the closure of an algebraic loop. By closing a loop, we ensure that the torn loop is correctly embedded in the causality graph as described in Section 4.1.2. The inverse process is denoted as opening of an algebraic loop. More details can be found in the work of Zimmer.<sup>13</sup>

#### 4.4. Fake residuals

In a dynamic system, algebraic loops may not only appear; they also may disappear. Unfortunately, this is not so easy to handle. The problem is that once the assumption of a tearing variable is established, it is maintained even when it becomes superfluous. The resulting tearing is by no means wrong, it just turns out to be partly redundant. Fortunately, there is a mechanism to detect potentially unnecessary tearings: the appearance of fake residuals.

Fake residuals are residual equations that could be causalized even without one of the corresponding tearing vectors. Therefore these residuals are avoidable and should not be part of an algebraic loop. Let  $\rho_f$  be a residual and  $r_f$  its relation. Consequently,  $U(r_f)$  is the set of corresponding

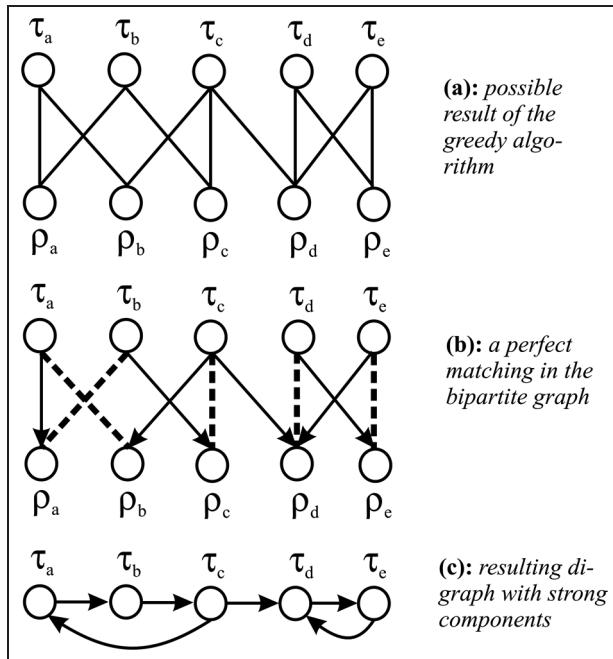


**Figure 15.** Optimal decomposition of the bipartite graph using perfect matching.

potential unknowns, and  $D(r_f)$  represents all its additional variables. The residual  $\rho_f$  is a fake residual, if there exists an open tearing  $\tau$  so that  $\tau$  is a predecessor of  $r_f$ , and only one of its potential unknowns, in  $U(r_f)$  is dependent on  $\tau$  as well as no other variable in  $D(r_f)$ . In order to remove a fake residual, the corresponding tearing  $\tau$  is removed, and all intermediate relations are decausalized, as is done for the removal of potential paths.

Some bad tearings (but not all of them) include fake residuals. The existence of a fake residual always enables optimization. At least, the size of the tearing block can be reduced by the fake residual itself, but it is likely that even the number of residuals can be reduced.

Fake residuals should be detected and removed before the residual causes any other action. The elimination of fake residuals ensures that forward causalization is always applied to the maximum extent. Please note also that fake residuals do not only occur at structural changes; they may even be generated through a non-ideal selection of tearing variables. Thus, the detection and removal of fake residuals helps avoid redundant and bad tearings. In this way, the simple heuristics for the selection of tearing variables can be partly improved in those cases where too many tearing variables have been generated.

#### 4.5. Integration of the tearing algorithms

We need to still clarify, how the proposed tearing algorithms are integrated into the whole process of dynamic

DAE processing. As an illustration, we use the flow chart in Figure 16.

The flow chart contains all major parts of the dynamic framework, let that be forward causalization, tearing or the evaluation of relations. To understand this chart, we have to consider it as part of a processing loop: each time we finish one task, we reiterate again from the start until the complete system has been validated or an error has been detected.

At the start of each iteration, we have to determine the main objective first. To this end, there are four decisions on the left-hand side of the flow chart that prioritize the major subprocesses. Let us take a brief look at each of those subprocesses.

1. Most important is to process all new relations. This includes relations, the causality of which has been removed and that have been reset from the system, as this happens by the removal of a potential path (see Section 3.4).
2. Residuals are processed in order to detect potentially causalized paths or to close an algebraic loop. The matching algorithm may detect an overdetermination.
3. Relations that have been causalized but not yet evaluated are ready for evaluation now. Please note that the evaluation of subparts of the system may cause structural changes, i.e. relations are removed or new relations are entered into the system.
4. At last, tearing variables are selected in order to causalize parts that are still non-causalized. The presence of open tearings indicates underdetermination.

In general, this enhanced processing scheme still follows the spirit of Section 3. Forward causalization is the dominant process, and conflicts are analyzed and resolved by means of residuals.

A final remark about Figure 16. The presented flow chart is of course simplified. Other valid schedules of the subtasks are thinkable as well. Indeed, the actual implementation of Sol differs from this flow chart for reasons of efficiency, but, aside from adding complexity, this does not provide any further insight.

#### 4.6. Asymptotic complexity

It has yet to be shown that the proposed algorithms for algebraic loops and their integration into the DDP yield a correct solution for index-one systems. Although we cannot formally prove this, we at least have a very strong indication for this to be true.

We know that index-zero systems are properly handled. Adding tearing relations to the system is per se nothing harmful, even if the chosen tearing variables turn out to be redundant. The ongoing detection and removal of fake

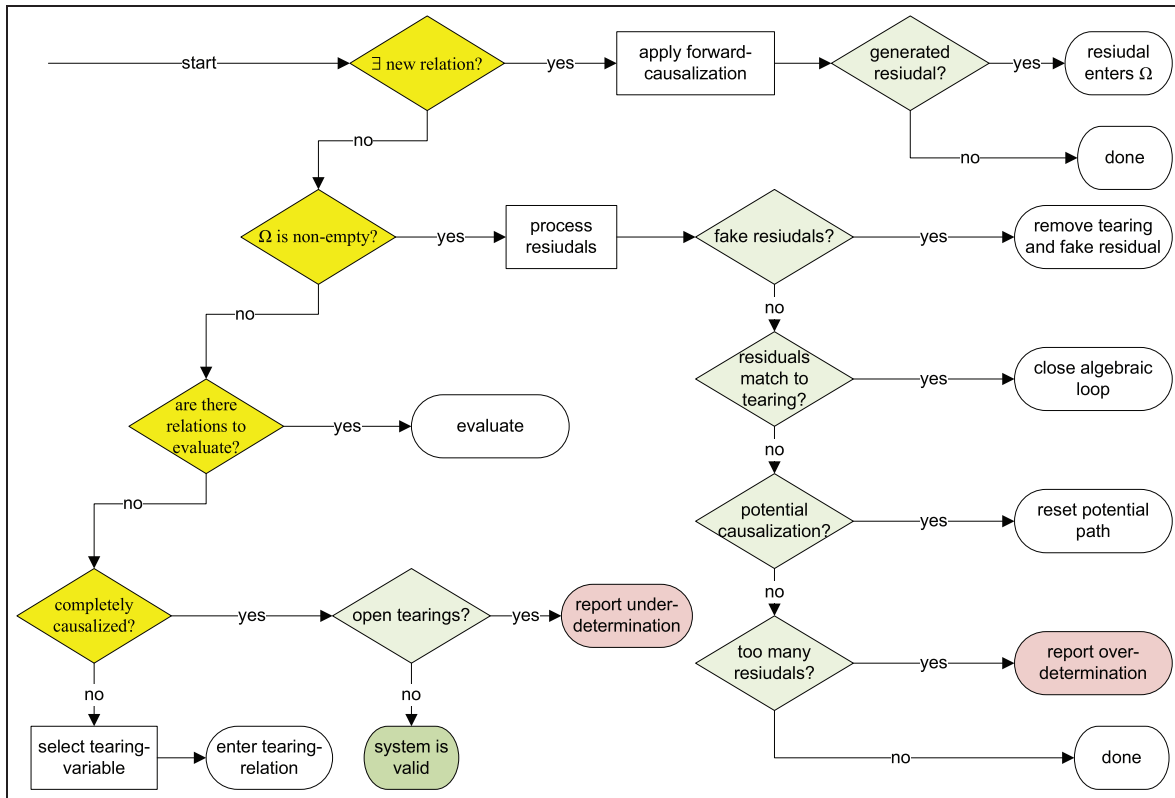


Figure 16. Processing of relations in the dynamic framework.

residuals ensures furthermore that forward causalization is always pursued to maximal extent. This means that each variable is only chosen as tearing variable, because it could not be determined by forward causalization. This helps to keep the number of tearing variables small. In a regular system, the number of resulting residuals will match the number of tearing variables.

It is not evident that the tearing process will terminate, since one may fear that the removal of fake residuals with their corresponding tearings and the subsequent reset of causalizations (leading to a new tearing) could lead to an infinite loop.

First of all, the selection of a tearing variable cannot generate a fake residual that leads to its own removal, since forward causalization is performed before any new tearing variable is chosen. A tearing can only cause fake residuals for the removal of tearings that have been selected earlier.

Let us therefore remember that a fake residual ensures by definition that it can be causalized by forward causalization and potentially many more relations can be causalized with it. There might still be a need to replace the removed tearing by a new one. Nevertheless, the non-causalized subset of relations for the new tearing relation will be strictly smaller than it was for the removed one. If a potential replacement tearing only causalizes this subset again (or less), it cannot cause any further fake residuals.

If a potential replacement tearing causalizes more than this subset, it could cause further fake residuals but thereby the causalization of the systems has to advance. In a finite system, this cannot happen infinitely often. Hence, this process will terminate.

Theoretically, a frequent occurrence of fake residuals could lead to an inefficient handling of the DAE system. In practice, however, that problem never occurred. In general, the system is able to process most systems and their structural changes rather quickly, because of its ability to restrict the changes to only those parts that are indeed affected. The processes for the closing and opening of algebraic loops are in  $O(|V_G| + |E_G|)$ . The same holds true for the heuristics of the selection of tearing variables.

The detection of fake residuals works practically in constant time. The subsequent removal is also in  $O(|V_G| + |E_G|)$ . The cost for the matching of residuals to their corresponding tearings is polynomial, and the algorithms are performed on a much smaller problem size.

Certain structural changes, however, may be treated in an inefficient way. For instance, the exchange of a simple equation within an algebraic loop by a structurally equivalent equation will cause the opening and closing of the complete algebraic loop. If the loop is large, the costs can be substantial. The current strategy represents to some degree an overhasty approach. This requires an

improvement since the switching of equations occurs frequently within algebraic loops.

#### 4.7. Detecting singularities

The primary task of the DDP is to enable the simulation of regular DAEs with structural changes. No less important, however, is its second task: Detecting singularities in the model. In the given framework, we can distinguish between two types of singularities that will yield error reports.

- Non-temporary underdetermination.
- Overdetermination.

**4.7.1. Detecting over- and underdetermination.** The detection of over- and underdetermination is located in the process flow of Figure 16.

Overdeterminations are detected whenever residuals are processed. The greedy matching algorithm may find that residuals are not dependent on any tearing variable or that a residual vector is dependent on a smaller vector of tearing variables.

Underdetermined systems of equations will result in open tearing that cannot be closed. The underdetermined subsystems are specified by the components in the corresponding bipartite graph. All of those relations that are successors of an open tearing are part of the underdetermined system.

Since underdetermination represents an intermediate state of many structural changes, one shall report them only when no further relations are scheduled for evaluation. This is why their detection is placed at the end of the priority queue in Figure 16.

## 5. Higher-index systems

### 5.1. Differential-index reduction

The preceding two sections dealt only with models where each statement of a derivative resulted in a state variable for time integration. This implicit assumption, however, only holds true for a rather simple class of models. In particular, the object-oriented design of model components requires the statement of many derivatives, where only a subset of them can represent state variables since many potential state variables are related by algebraic constraints. For variable-structure systems, this means that the exchange of a single equation can change the number of state variables, even if the equation itself does not contain any derivative. Figure 17 illustrates a corresponding example.

The half-way rectifier with line inductance is a well-known circuit, and there are many solutions available that handle the structural change in a highly efficient manner. For instance, inline integration<sup>32</sup> can be applied. Yet, let us refrain from specific solutions and look at the problem in general.

The structural change in this model is caused by the ideal diode. In Listing 4, its state is described by the Boolean variable `open` that represents the two possible modes.

```

1  model HWRLI
2  implementation:
3    //declarations are omitted    [...]
4    i0 = iC+iR;
5    iC = C*der(uC);
6    uC = R2*iR;
7    u0 = sin(x = time*100*pi)
8    uR = R1*i0;
9    uL = L*der(i0);
10   u0 + uR + uD + uL = uC;
11   static Boolean open;
12   when uD<0 then
13     open << true;
14   end else when i0>0 then
15     open << false;
16   end;
17   if open then
18     uD = 0;
19   else then
20     i0 = 0;
21   end if;
22 end HWRLI;

```

**Listing 4.** Flat Sol model of a half-way rectifier.

The switch between the modes is triggered by a corresponding when-statements, whereas the actual exchange of the continuous-time equations is modeled by the if-branch. For both directions, the change is expressed by  $\dot{s} = (\{r_{18}, r_{20}\}, \emptyset)$ .

If the diode is closed, the voltage across the diode is zero, and the system contains two state variables for time integration: `uC` that represents the voltage across the capacitor and `i0` that represents the current through the inductor. In the open mode, the current is not a state variable any more since it is set to zero by the diode. In order to determine the voltage across the inductance, the derivative of the current `i0` is required. In this model, the derivative is obviously zero.

This model of a half-way rectifier is an example of a system with variable differential index.<sup>33</sup> The differential index denotes the number of differentiations that are required in order to transform the DAE into a form suitable for numerical ODE solvers. In this example, one differentiation is sufficient, and hence the differential index varies from zero to one. Mostly, systems of DAEs are characterized by the *perturbation index*.<sup>17</sup> Roughly speaking, the perturbation index of a system equals the differential index if there are no algebraic loops as in this example. Otherwise, it is larger by one.

### 5.2. Index reduction by Pantelides

Typically, index reduction is performed by means of symbolic differentiation. The most common procedure for this task originates from the Pantelides algorithm.<sup>34</sup> This

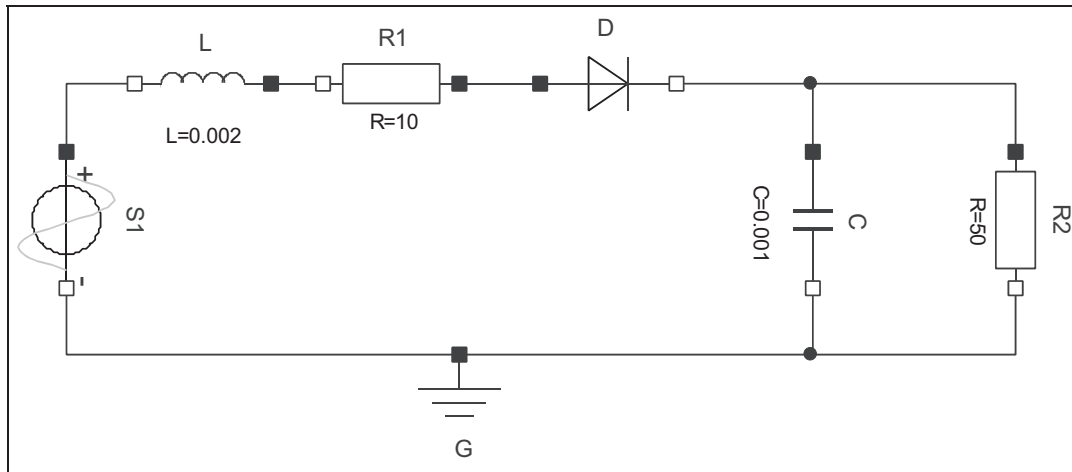


Figure 17. Half-way rectifier circuit.

method has been successfully applied in commercial software such as gPROMS or Dymola.

The Pantelides algorithm proposes that initially all potential state variables are assumed to be known. These are all of those variables for which time derivatives appear in the model. This assumption may result in overdetermined equations that give rise to so-called structural singularities. For each of these constraint equations, a corresponding integrator will be eliminated, and the constraint equations will be added to the system in its differentiated form. The elimination of the integrator will demand the recausalization of parts of the system. The differentiation of the constraint equation is likely to invoke further differentiations.

For the static treatment of DAEs, the Pantelides algorithm is often implemented in such a way that it works in alternation with the causalization of the DAEs. The causalization determines the constraint equations, and the Pantelides algorithm gets rid of this overdetermination again. This two-phase behavior is the main reasons why the Pantelides algorithm in this form is not suited for a dynamic framework. First, it generates potentially many residuals that are relatively expensive to handle and second, it requires restructuring of larger parts of the system. Thus, we prefer a different approach that suits the demands of our dynamic framework. Common with the Pantelides algorithm is that the index gets reduced by means of symbolic differentiation and the elimination of potential state variables.

### 5.3. Tracking symbolic differentiation and selection of states

Automatic symbolic differentiation of algebraic equations is a common problem and has been solved (in its classic form) long ago.<sup>35,36</sup> What remains problematic is to determine, which parts of the system need to be differentiated,

especially with respect to a dynamic framework. To this end, a set of update and downdate rules has been developed. The precise rules are contained in the work of Zimmer,<sup>13</sup> but essentially differentiated equations can be added to and removed from the global set equations and are not differently treated than all other equations.

In order to express the differential part of a DAE, we provide a special relation: the derivative relation. This relation is stated by using the expression  $der()$  as in  $a = der(x=b)$ . It simply expresses that  $a$  is the derivative of  $b$ .

Table 2 presents the four different states for the causalization of a derivative relation. In the previous sections, we simply assumed that a derivative relation is causalized as an integrator. Hence,  $a$  is supposed to be known, and  $b$  is determined by time integration. However, if  $b$  is determined by other parts of the DAE, the derivative relation has to act as a differentiator. In this case,  $a$  is the unknown, and a symbolic differentiation of  $b$  is requested. Derivative relations can also become part of an algebraic loop. Thus, when acting as a differentiator, the relation may also throw a residual.

Like any other relation, derivative relations are also integrated into the process of forward causalization. Figure 18 illustrates the corresponding state transition diagram for the causalization. Another particularity of the derivative relation is indicated in Table 2: a derivative relation is a

Table 2 States of a derivative relation.

State	Variables in $D(r)$	Unknown
Non-causalized	$D(r) = \{a,b\}$	none
Integrator	$D(r) = \{b\}$	$b$
Differentiator	$D(r) = \{a,b,db/dt\}$	$a$
Differentiator with residual	$D(r) = \{a,b,db/dt,\rho\}$	$\rho$

polymorphic object. Depending on its current state, it changes its set of variables. This is required since integrators shall have no predecessors in the causality graph. In this way, all integrators can be synchronized, a prerequisite for the application of multi-dimensional, implicit algorithms for time integration (such as DASSL<sup>37</sup>).

If a derivative relation acts as an integrator, we say that it defines a continuous-time state variable of the system. Figure 18 depicts two possible ways that lead to this state. Either the state variable is determined directly by forward causalization if their derivative is independent from the state itself. Alternatively, the state variable is externally selected. This selection is integrated into the DDP in a similar way as the selection of tearing variables.

- Whenever forward causalization terminates but there are still non-causalized derivative relations, one of these derivative relations is arbitrarily selected and determined as integrator. Then, forward causalization proceeds.
- Only when there are no non-causalized derivative relations, the selection of tearing variables will be applied as described in Section 4.

The selection of continuous-time states is now embedded in the DDP. Initially, the set of state variables is empty. This is a first key difference to the Pantelides algorithm. Then, the state variables will be gradually selected in alternation with forward causalization. During this process, differentiated equations may be added to the system. Finally, the whole system should be causalized.

**5.3.1. Example.** Let us review this process of index reduction by a very simple example. Listing 5 corresponds to the model code of an RC circuit with two parallel capacitors.

```

1 model ParallelCapacitors
2 implementation:
3   //declarations are omitted [...]
4   u0 = 10;
5   uR = R*iR;
6   i1 = C1*der(x=u1)
7   i2 = C2*der(x=u2)
8   iR = i1+i2;
9   u1 = u2;
10  uR + u1 = u0;
11 end ParallelCapacitors;

```

**Listing 5.** Flat Sol model of a simple RC-circuit.

Forward causalization can only causalize the relation  $r_4$ . There remain two non-causalized derivative relations. Consequently, the variable  $u_1$  is selected as state variable, and the corresponding derivative relation  $r_6$  is determined as integrator. The next run of forward causalization causalizes all remaining relations except  $r_8$ . Among them is the second derivative relation that is causalized as differentiator. Consequently, the derivative of  $u_2$  is requested, and the differentiated equations of Listing 6 are added to the system.

```

i1 = C1*d_u1;
i2 = C2*d_u2;
d_u1 = d_u2;

```

**Listing 6.** Flat Sol model of a simple RC-circuit.

There are now four non-causalized relations, none of them being a derivative relation. Hence the tearing method is applied. The variable  $d_u2$  is selected as tearing variable, and relation  $r_8$  generates the corresponding residual. The DDP of this system is now complete. The

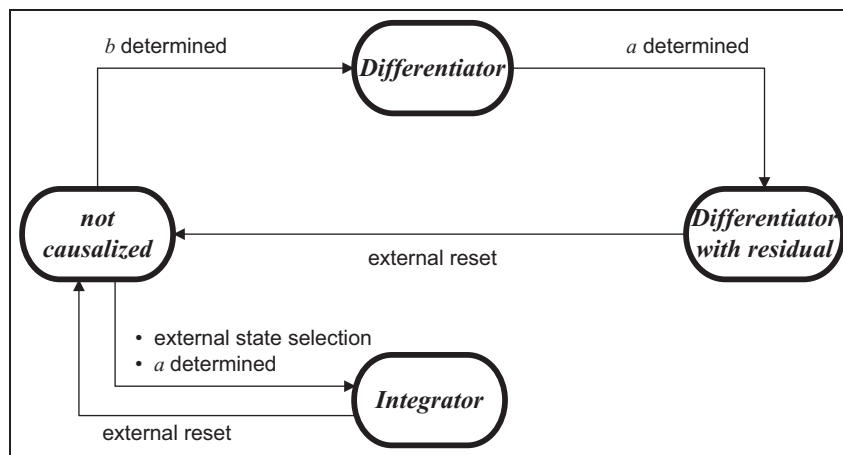


**Figure 18.** State transitions of derivative relations.

system has one continuous time state and there is a small system of equations that needs to be solved.

The selection of state variables can drastically influence the computational performance of a system, both in precision and efficiency. An automatic mechanism can hardly be expected to outperform the specific knowledge of a well-experienced modeler. Hence, some modeling languages, such as Modelica but also Sol, provide means for the modeler that enable him or her to suggest or prefer certain variables as state variables.

#### 5.4. Removing state variables

In a dynamic framework, structural changes may cause the number of state variables to change. Thus, we have to handle the removal of state variables as well. In principle, this follows the same principles as the removal of potentially causalized relations or the removal of tearing variables.

Too many state variables will result in an overdetermined system and yield residuals. In order to cope with these residuals, the sources of overdetermination will be examined. There are now three different kinds:

1. tearing relations;
2. potentially causalized relations;
3. state selections.

The list represents the priority with which these sources are being analyzed. In a first step, we examine the tearing relations as potential source of overdetermination. It is only if the matching algorithm of Section 4 detects an overdetermined subsystem that other sources must be removed.

In the case that both a potentially causalized relation and a state selection are potential sources of overdetermination, the potentially causalized relations are decausalized first. The reason for this is that potential causalizations shall only maintain existing causalization but not change the causality of other parts.

Hence, state variables get only deselected when they are the sole potential sources of overdetermination left. The deselection is achieved by decausalizing the corresponding derivative relations.

**5.4.1. Example.** The half-way rectifier with line inductance represents a simple example for the removal of state variables. If the diode is closed, the variable  $i_0$  is selected as state variable. The corresponding relation  $r_9$  acts as an integrator. The structural change exchanges relation  $r_{18}$  with  $r_{20}$ :  $i_0 = 0$  that is immediately causalized in residual form. The only source of overdetermination is the state selection and, therefore, the corresponding derivative relation gets decausalized. Forward causalization now causalizes  $r_9$ . This derivative relation determines

$u_L$  and acts now as a differentiator. Thus,  $r_{20}$  is being differentiated.

#### 5.5. Asymptotic complexity

The removal of state variables in Sol follows the general pattern of the DDP. In order to undo an existing causality, a corresponding conflict must occur in form of a residual. Since such a residual has now many potential sources of overdetermination, we presented a strategy by prioritizing the sources of overdetermination. This priority list, however, represents an arbitrary, heuristic decision. It is not a general solution. We can demonstrate for a broad set of examples (electrical circuits and planar mechanical systems) that this strategy works fine, but it may fail for other examples.

With respect to algorithmic complexity, the outlined process of state selection and removal does not introduce any new, computationally expensive processes. We know that all costly processes are associated with residuals. Hence, the outlined strategy for state selection avoids the generation of residuals whenever possible. In contrast to the Pantelides algorithm, potential state variables are supposed to be unknown and are only successively chosen as states when necessary.

In Section 4, we could show that the removal of tearing variables will not lead to an infinitely self-repeating process. Unfortunately, the same cannot be stated for the undoing of state selections. It is therefore necessary to keep track of the selected states during a structural change. More research is needed to find a better, truly general strategy for higher-index systems.

Another key point with respect to efficiency is the differentiation of equations. In order to prevent overhasty actions, the instantiation of derivatives is done in busy form, whereas the removal is done in lazy form. This shall avoid unnecessary re-instantiations.

#### 5.6. Summary

The complete DDP is composed out of many different algorithms and rules that are linked with each other in a highly elaborate way. The actual software implementation involves further details that have been omitted here for brevity. Despite this high degree of complexity, there is a common principle covering all important subtasks. In summary, the methodology of the DDP can be presented as follows.

Forward causalization is the dominant strategy. If it does not suffice alone, it is assisted by the selection of state variables and tearing variables. Furthermore, existing causalizations are protected from overhasty removal by the concept of potentially causalized relations. These three additional means form a potential source of overdetermination. Hence, whenever a residual is created, the potential

sources for the overdetermination are examined, and a corresponding action is taken in order to remove the conflict.

## 6. Validation

In this section, the proposed computational framework is being evaluated. To this end, we apply the prototype Simulator Solsim to two examples.

One obvious evaluation criterion is the computational efficiency of the prototype implementation. Although, the examples in this section demonstrate that the simulator speed is sufficient to perform meaningful simulations, the simulator is of course not very efficient, simply because it represents an interpreter (in contrast to a compiler such as Mosilab). Hence, for any specific simulation task at hand, it is always possible to provide a manually coded solution that significantly outperforms the Solsim simulator. It is important to note, that there is no optimal computational framework for variable structure systems in general. This question can only be answered for a specific system at hand.

For the evaluation of this research work, other factors are more important than the speed of its prototype implementation. In this section we focus on three criteria.

- **Generality:** is the framework able to handle general classes of equation-based models?
- **Scalability:** does the computational framework scale? Does it extend to problems with many thousands of equations?
- **Extendability:** How can the proposed technology be combined with other approaches, leading to more powerful frameworks in the future?

The first two criteria are discussed by means of examples. The last one is discussed by giving a short outlook on potential future work.

### 6.1. Example 1: Examining the generality by revisiting the trebuchet

A prime test application for the Sol framework is the trebuchet catapult from the introduction. To this end, a planar mechanical library has been developed in Sol. In addition to the continuous-time equations (from that a few excerpts have been shown), the components of this library contain a second set of discrete equations that model the impulse behavior. In fact, every force impulse causes a discrete change in velocity is therefore modeled as small, temporary structural change.

The components have been assembled as outlined in Figure 3. The total system contains roughly 250 equations and represents an index-three system. A major subset of equations need to be differentiated twice and there remain two linear algebraic equation-systems to be solved. The

handling of the occurring structural changes is consequently difficult and requires all capabilities of Solsim. Including the structural changes for the force impulses, a total of six structural changes occur during the first two seconds of simulation. Whereas the processing of equations is highly elaborate in Sol, its numerical methods are still very rudimentary. Hence, 2000 steps of forward Euler have been applied. Yet the whole simulation, from parsing to simulation output, could be performed roughly within one second on a common, contemporary PC.

Being able to simulate the trebuchet means being able to simulate a large class of models. Modeling of continuous process, modeling of discrete processes, higher-index problems: the trebuchet contains it all. Limitations in generality still may originate from difficult higher-index problems, where the implemented prototype still lacks the required robustness. Also the event-based modeling is very simple and is not able to cover all needs that occur in the modeling of physical systems.

The trebuchet demonstrates that Sol provides a very general framework. The benefit of this generality is to the modeler. It enables to spread the formulation of structural changes among several distinct components. These components form a planar mechanical library whose entities are reusable and could be reassembled to other mechanical devices. Without this level of generality, the structural changes would have to be formulated in a central way and the resulting code would not be generic.

The trebuchet is not suited to show the value of the incremental update approach. Since the structural changes affect mostly large fractions of the system, a complete recausalization at each change is of roughly the same speed. Hence, let us look at another example.

### 6.2. Example 2: Examining scalability by modeling population dynamics with genetic adaptation

In this application, we wish to model the rise and fall of an abstract life form that thrives on a finite, global nutrition and thereby transforms it into a global pollutant. An example for such a life form could be yeast in a fermentation tank that consumes sugar and poisons itself with the resulting alcohol. Any life form needs energy to sustain its metabolism. This is obtained from the nutrition. We suppose that the energy increment is proportional to the intake of nutrient  $f$ , and that the intake itself is proportional to the concentration of the nutrient  $c_N$ . This is specified by the parameters for the scope  $s$  of the life form and its absorbance  $r$ :

$$f = c_N s r$$

The intake of nutrient will be proportional to the reduction of its concentration as well as to the increase of pollution  $c_P$ :

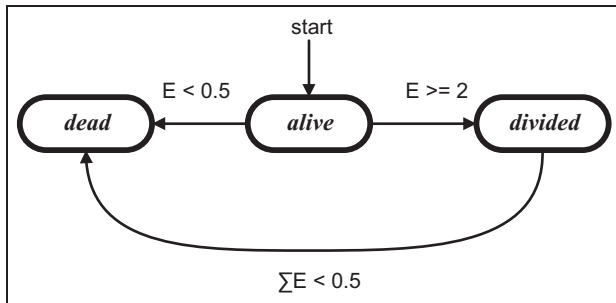


Figure 19. Modes of the reproductive life form.

$$\dot{c}_N = \dot{c}_P \propto -f$$

We suppose furthermore that the life form is able to store energy within its metabolism. Its current energy level is represented by the variable  $E$ . The unit of this variable is defined such that the value 1.0 represents the initial energy of a life form. The inflow of nutrition is transformed into power by the coefficient  $\mu_E$ . Since energy is needed to maintain the metabolism, we suppose that this is a constant value  $M$ . Another sink of energy is caused by the concentration of the pollutant  $c_P$ . The corresponding sensitivity is arbitrarily defined to be quadratic and is parameterized by  $\mu_{c_P}$ . This leads to the following differential equation for the energy level:

$$\dot{E} = f\mu_E - M - \mu_{c_P}c_P^2$$

In dependence on this energy level, the life form is enabled to reproduce itself, and it is forced to die at a minimum energy level. This goes along with a genetic adaptation of its offspring to the environment. For the reproduction, we select a non-sexual model that mimics cell division. Each life form has three potential modes:

alive, divided, and dead. Initially, a life form is alive with an energy level of 1.0. The transition to one of the other modes is then triggered by a change in the energy level. The life form dies when its energy level sinks below 0.5. It divides when the energy level rises above 2.0 (Figure 19).

The adaptation process concerns the absorbance and represents a trade-off between feeding and resistance. To this end, the absorbance is coupled with the sensitivity of the pollutant by the equation

$$\mu_{c_P} = 0.5 + \mu_E r^2$$

At each division, the absorbance of one of the two life forms is randomly modified within the uniform range of  $\pm 10\%$ . A higher absorbance leads to a higher nutrition level and the ability to reproduce faster than the competitors. On the other hand, the high absorbance rate makes the life form more vulnerable and decreases its ability to survive in a polluted environment. Which of these capabilities is more important is determined by the environment.

The resulting Sol model consist of roughly 100 code lines and the output of the corresponding simulation is shown in Figures 20 and 21. Initially, one single life form is put into a tank with 1000 liters of volume and a nutrition concentration of 20%. At the beginning, the population is rising exponentially. This rise looks almost like a perfectly continuous exponential curve but a closer look reveals the discrete character that is introduced by the reproduction cycle. Together with the population also the pollution is rising and puts a rather sudden end to the growth. The population reaches a plateau and pauses, before die-off sets in.

Figure 21 depicts the genetic evolution of the absorbance  $r$ . At the beginning, there is plenty of nutrition, and a higher absorbance enables a shorter reproduction cycle. This naturally leads to an increase in the mean absorbance. However, also life forms with low absorbance can still

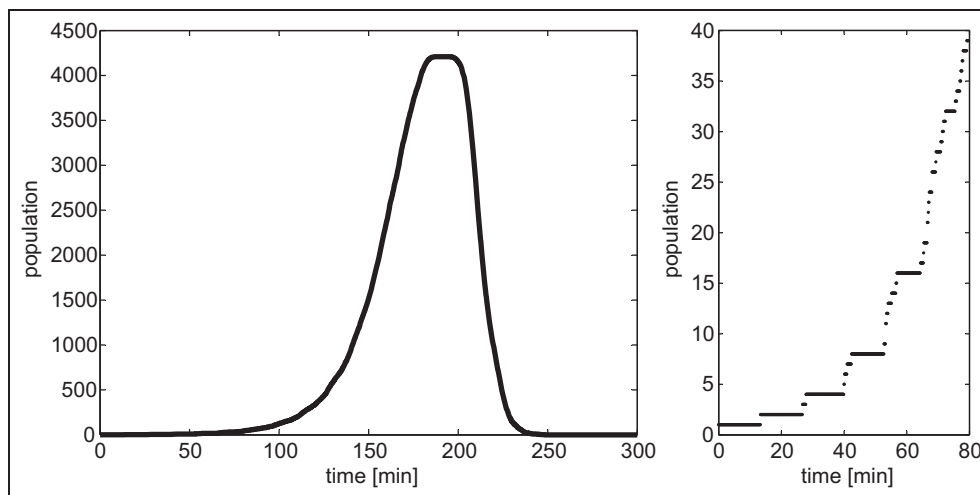


Figure 20. Population size with magnification.

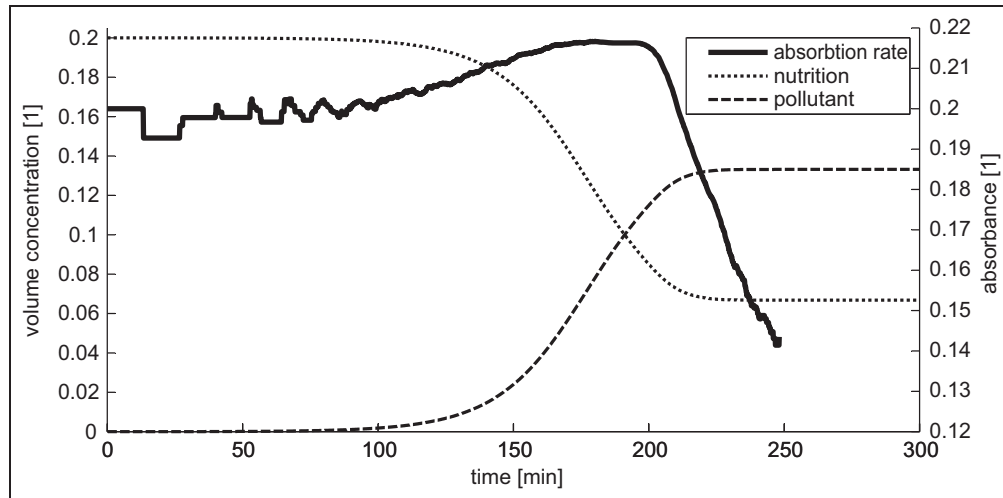


Figure 21. Mean absorbance with respect to nutrition.

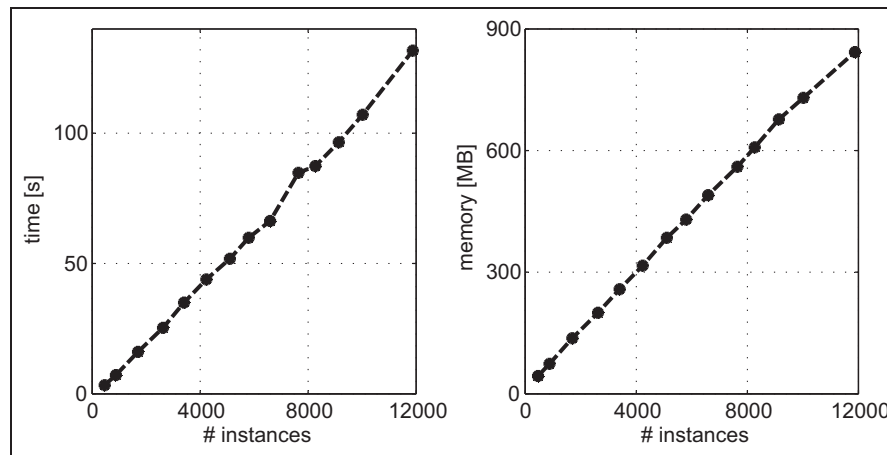


Figure 22. Scaling performance of Sol.

thrive in this environment. Owing to the exponential growth that is induced by the self-reproduction, the change in nutrient concentration is rather sudden, and the pollution resistance becomes the key factor. Life forms with a high absorbance are vulnerable and become victims of their own success. A lower absorbance is now strongly favored and those life forms remain alive for a while. Nevertheless, the relation between nutrition and pollution forms already a very hostile environment that finally results in total extinction. Some of the nutrition remains unused.

The simulation of this system is very interesting with respect to its computational aspects. Whereas the model definition is small, the resulting size of the simulation can be huge. In this example, the population peaks around 4200 living life forms. Hence, the total system contains several thousands of state variables and about 100,000

relations. During simulation, about 10,000 events are being triggered.

Here the incremental update algorithm pays off. Each structural change only affects between 10 and 25 equations and can be handled locally. In this way the computational load of structural changes accounts for only 4.5% of the complete simulation time whereas a complete recausalization at each change would cause a load of roughly 80% of the simulation time. Also this model is very well suited to test how the performance scales with respect to the model size. To this end, the simulation was performed for different volume sizes with computational time and memory effort being recorded. Figure 22 shows the corresponding results with respect to the number of model instances. Evidently, the performance of Solsim scales linearly to the problem size. This is certainly optimal and corresponds to the performance analysis of Section 3.

The implementation of Solsim, however, does contain parts that behave worse than linear performance. Fortunately, these parts do not dominate the simulation and their influence is covered up by the main processes. The memory overhead of Solsim is quite significant: roughly 3.5 MB are needed per 1000 relations. This is certainly a lot, and there is definitely much potential for further optimizations. Compared with other translators of equation-based languages, this memory effort is not exceptional. The memory usage of the Modelica translator in Dymola is of the same order of magnitude with an estimated 1–2 MB per 1000 relations.<sup>38</sup>

### 6.3. Examining the future potential

Examples 1 and 2 showed the general feasibility of the approach in the sense that higher-index problems can be treated and that also a larger model can be handled. Two more examples are included in the work of Zimmer.<sup>13</sup>

The efficiency of the handling of structural changes can be measured by relating the corresponding computational effort to the overall computational effort for the complete simulation. For both examples, the incremental algorithms require less than 5% of the total simulation time (1.5% for the trebuchet and 4.5% for the population dynamics example). Hence, one might be tempted to state that the handling of structural changes is very efficient but this conclusion is flawed since the ODE-Simulator in Sol is not a good point of comparison. First, the function evaluation is done by an interpreter and second, an excessively large number of steps are enforced by applying Forward Euler instead of higher-order methods.

The good news is that if you can afford that your system is being interpreted, you can also afford to simulate structural changes but it is also true in cases where an interpretation is feasible, a complete recausalization (avoiding the incremental algorithms) is often feasible as well. So what is the precise motivation for the incremental algorithms then?

For the static case, the classic method of index reduction is a key factor to simulation performance since it enables the compilation and optimization of simulation code in advance. In future, it is also the goal that the code of variable structure system can be compiled at least in parts and probably just-in-time (JIT). Now the importance of the proposed incremental algorithms for structural changes becomes evident. Since the effect of a structural change can be contained to a part of the system, a complete recompilation of the system can be avoided and large fractions of already compiled code can be reused.

The efficient application of JIT compilers for variable structure systems has already been demonstrated by Nilsson et al.<sup>11,12</sup> This work contains a notable complementary approach to the Sol framework. Ideally, the incremental algorithms proposed in this paper might then be used to identify the affected code pieces and generate the

index reduction for the new code in place. This of course opens up another research field. How to determine an optimal decomposition of the system in separately compiled functions, when to cache compiled code, and when to generate code for many mode changes in advance are interesting research questions that yet need to be answered.

For the current state of the art, Sol has successfully demonstrated how to express and simulate DAE-based variable structure systems in a very general way.

## 7. Conclusion

The dynamic processing of DAEs enables the modeling and simulation of complex systems with arbitrary structural changes. Sections 2 and 3 introduced the general framework. They presented the causality graph as a fundamental data structure as well as the concepts of forward causalization and potential causalization. Sections 4 and 5 provided additional functionality for index reduction. The system is now able to cope with algebraic loops and to enforce differentiation for the purpose of index reduction.

The resulting DDP represents an almost general solution. It is perfectly suited for index-zero systems, it works fine for index-one system with algebraic loops, and it represents a practical (but incomplete) solution for higher-index systems.

The dynamic processing scheme enables also new modeling techniques that are represented by the corresponding language Sol. The population dynamics example and the trebuchet model demonstrate the usefulness of this approach. Altogether, we provided a complete, dynamic framework for the equation-based modeling of variable-structure systems. In this way, we have entered a new and promising field for future research that lets us and other researchers elaborate new modeling and processing techniques. We hope that the research field can establish itself and will lead to improved industrial standards for equation-based modeling in the future.

## Acknowledgments

I would like to thank Professor François E. Cellier and Professor Walter Gander for their helpful advice and their continuing support.

## Funding

This research project was generously sponsored by the Swiss National Science Foundation (SNF Project No. 200021-117619/1) and co-funded by the Department of Computer Science at ETH Zurich.

## References

1. Fritzson P. *Principles of Object-oriented Modeling and Simulation with Modelica 2.1*. New York: John Wiley & Sons, 2004.

2. The Modelica Association. <http://www.modelica.org>
3. Ashenden PJ, Peterson GD and Teegarden DA. *The System Designer's Guide to VHDL-AMS*. San Mateo, CA: Morgan Kaufmann, 2002.
4. Oh M and Pantelides CC. A modelling and simulation language for combined lumped and distributed parameter systems. *Comput Chem Engng* 1996; 20: 611–633.
5. Fábrián G. *A Language and Simulator for Hybrid Systems*. PhD Thesis, University of Technology, Eindhoven, The Netherlands, 1999.
6. van Beek DA. Variables and equations in hybrid systems with structural changes. In: *Proceedings of the 13th European Simulation Symposium*, Marseille, 2002, pp. 30–34.
7. Nytsch-Geusen C, Ernst T, Nordwig A, et al. Advanced modeling and simulation techniques in MOSILAB: a system development case study. In: *Proc. 5th International Modelica Conference*, Vienna, Austria, Vol. 1, 2006, pp. 63–71.
8. Mosterman PJ. HYBRISIM – a modeling and simulation environment for hybrid bond graphs. *J Syst Control Engng* 2002; 216: 35–46.
9. Roychoudhury I, Daigle M, Biswas G and Koutsoukos X. Efficient simulation of hybrid systems: an application to electrical power distribution systems. *SIMULATION* 2011; 87: 467–498.
10. Giorgidze G and Nilsson H. Higher-order non-causal modeling and simulation of structurally dynamic systems. In: *Proceedings of the 7th International Modelica Conference*, Como, Italy, 2009.
11. Nilsson H, Peterson J and Hudak P. Functional hybrid modeling from an object-oriented perspective. In: *Proceedings of the 1st International Workshop on Equation-Based Object-Oriented Languages and Tools (EOOLT)*, Berlin, Germany, 2007, pp. 71–87.
12. Nilsson H and Giorgidze G. Exploiting structural dynamism in functional hybrid modelling for simulation of ideal diodes. In: *Proceedings of EUROSIM 2010*, 2010.
13. Zimmer D. *Equation-Based Modeling of Variable-Structure Systems*. PhD Dissertation No. 18924, ETH Zürich, Switzerland, 2010.
14. Zimmer D. An application of Sol on variable-structure systems with higher index. In: *Proceedings of the 7th International Modelica Conference*, Como, Italy, 2009.
15. Zimmer D. Introducing Sol: a general methodology for equation-based modeling of variable-structure systems. In: *Proceedings of the 6th International Modelica Conference*, Bielefeld, Germany, Vol. 1, 2008, pp. 47–56.
16. Dassault Systemes. [www.dynasim.se](http://www.dynasim.se).
17. Bujakiewicz P and van den Bosch PPJ. Determination of perturbation index of a DAE with maximum weighted matching algorithm. In: *Proceedings of the IEEE/IFAC Joint Symposium on Computer-Aided Control System Design*, Tuscon, AZ, 1994, pp. 129–135.
18. Bujakiewicz P. *Maximum Weighted Matching for High Index Differential Algebraic Equations*. PhD Thesis, Technische Universiteit Delft, 1993.
19. Widmayer P and Ottmann T. *Algorithmen und Datenstrukturen, 4. Auflage*. Spektrum Akademischer Verlag, 2002.
20. Pearce DJ and Kelly PHJ. A dynamic algorithm for topologically sorting directed acyclic graphs. In: *Experimental and Efficient Algorithms (Lecture Notes in Computer Science, Vol. 3059)*. Berlin: Springer-Verlag, 2004, pp. 383–398.
21. Katriel I and Bodlaender HL. Online topological ordering. In: *Proceedings of the ACM-SIAM Symposium on Discrete Algorithms (SODA)*, 2005, pp. 443–450.
22. Tarjan R. Depth-first search and linear graph algorithms. *SIAM J Comput* 1972; 1: 146–160.
23. Cellier FE and Kofman E. *Continuous System Simulation*. New York: Springer-Verlag, 2006.
24. West DB. *Introduction to Graph Theory*, 2nd ed. Englewood Cliffs, NJ: Prentice Hall, 2001.
25. Steward DV. Partitioning and tearing systems of equations. *J SIAM B Numer Anal* 1965; 2: 345–365.
26. Pothén A and Fan C. Computing the block triangular form of a sparse matrix. *ACM Trans Math Softw* 1990; 16: 303–324.
27. Campbell SL and William C. The index of general nonlinear DAEs. *Numer Math* 1995; 72: 173–196.
28. Richard S and Mah H. *Chemical Process Structures and Information Flows*. London: Butterworth, 1990.
29. Golub GH and Van Loan CF. *Matrix Computations*, 3rd ed. Baltimore, MD: The John Hopkins University Press, 1996.
30. Upadhye RS and Grens EA. An efficient algorithm for optimum decomposition of recycle systems. *AIChE Journal* 1972; 18: 533–439.
31. Ollero P and Amselem C. Decomposition algorithm for chemical process simulation. *Chem Engng Res Des* 1983; 61: 303–307.
32. Cellier FE and Krebs M. Analysis and simulation of variable structure systems using bond graphs and inline integration. In: *Proceedings of ICBGM'07, 8th SCS International Conference on Bond Graph Modeling and Simulation*, San Diego, CA, 2007, pp. 29–34.
33. Leimkuhler B, Gear CW and Gupta GK. Automatic integration of Euler–Lagrange equations with constraints. *J Comp Appl Math* 1985; 12–13: 77–90.
34. Pantelides C. The consistent initialization of differential-algebraic systems. *SIAM J Sci Stat Comput* 1988; 9: 213–231.
35. Gander W. *Computer Mathematik*. Basel: Birkhäuser Verlag, 1985.
36. Joss J. *Algorithmisches Differenzieren*. PhD Thesis, ETH Zürich, Switzerland, 1976.
37. Petzold LR. A description of DASSL: a differential/algebraic system solver. *IMACS Trans Sci Comput* 1983; 1: 65.
38. Zimmer D. Multi-aspect modeling in equation-based languages. *Sim News Eur* 2008; 18(2): 54–61.

### Author biography

**Dirk Zimmer** received his PhD degree at the Swiss Federal Institute of Technology (ETH). He is currently pursuing his research work at the Institute of System Dynamics and Control belonging at the German Aerospace Center (DLR). In addition, he is lecturer at the Technical University of Munich (TUM).